

TA7
E8
no.ERDC/GSL
TR-08-22
c.2

LIBRARY
USE ONLY



**US Army Corps
of Engineers®**
Engineer Research and
Development Center

Risk Assessment of Rock Surface Spillway Erosion Using Parametric Studies

Evelyn Villanueva and Johannes L. Wibowo

September 2008



US - CE - C
PROPERTY OF THE UNITED STATES
GOVERNMENT

ERDC/GSL TR-08-22
September 2008

Risk Assessment of Rock Surface Spillway Erosion Using Parametric Studies

TA7
E8
no. ERDC/GSL
TR-08-22
C.2

Evelyn Villanueva and Johannes L. Wibowo

Geotechnical and Structures Laboratory
U.S. Army Engineer Research and Development Center
3909 Halls Ferry Road
Vicksburg, MS 39180-6199

Final report

Approved for public release; distribution is unlimited.

RESEARCH LIBRARY
USACE ERDC
VICKSBURG, MS

Prepared for Headquarters, U.S. Army Corps of Engineers
Washington, DC 20314-1000

Abstract: As more dams experience spillway flows from flood events, identification and analysis of erosion in auxiliary rock surface spillways has become a primary focus in maintaining dam integrity. The spillway erosion risk assessment developed for this research is based on parameters identified and discussed in previous research as the leading factors influencing spillway damage from erosion.

Parameters applied in this analysis were channel geometry, stream hydrology, and geologic materials. Channel geometry is described by the length of spillway channel and slope of the spillway floor; stream hydrology is classified by the peak discharge and its duration; and geologic material is identified by its behavior in resisting erosion.

The Sites Spillway Erosion Analysis (SSEA) was used to produce a risk assessment based on U.S. Army Corps of Engineers case histories. The risk assessment was used to classify and refine model uncertainties, an important advancement in evaluating spillway erosion.

DISCLAIMER: The contents of this report are not to be used for advertising, publication, or promotional purposes. Citation of trade names does not constitute an official endorsement or approval of the use of such commercial products. All product names and trademarks cited are the property of their respective owners. The findings of this report are not to be construed as an official Department of the Army position unless so designated by other authorized documents.

DESTROY THIS REPORT WHEN NO LONGER NEEDED. DO NOT RETURN IT TO THE ORIGINATOR.

Contents

Figures and Tables	iv
Preface	vi
1 Introduction	1
2 Previous Studies	3
USDA model.....	4
Erosion models threshold line.....	6
Threshold zone.....	12
Erodibility index.....	15
Material strength number (M_s).....	15
<i>Material strength number of cohesionless soil</i>	16
<i>Material strength number of cohesive soil</i>	17
<i>Material strength number of rock</i>	17
Block/particle size number.....	18
Discontinuity bond shear strength number.....	20
Relative ground structure number.....	21
3 Problem Statement	24
4 Methodology	26
Parametric study data and SSEA.....	26
Influence of particle diameter in vertical erosion.....	26
Parameters selection.....	29
Summary of examples using SSEA.....	30
5 Results and Discussion	33
Probability.....	33
Linear regression.....	33
Logistic regression.....	36
Ordinal regression.....	39
Case history data application.....	40
6 Conclusions	43
References	44
Appendix A: Probability of Damage Comparing SSEA and Ordinal Logistic Regression (OLR) Results	47
Report Documentation Page	

Figures and Tables

Figures

Figure 1. The three phases of headcut erosion (after USSD 2004).	4
Figure 2. Critical stress for incipient motion calculated from Shield's criteria used in Phase 2 (USDA, NRCS 1997).	6
Figure 3. Sketch of threshold line concept showing stream power versus erodibility index (Wibowo et al. 2005).	7
Figure 4. Threshold line developed by USDA (Moore et al. 1994).	9
Figure 5. Curve for determination of headcut advance rate coefficient (Temple and Moore 1994).	11
Figure 6. Annandale's threshold line (Annandale 1995).	12
Figure 7. Threshold zone developed from USACE erosion data points (Wibowo and Murphy 2005).	13
Figure 8. Damage to Canyon Lake Spillway during and after a storm event in July 2002 (photos courtesy USACE District, Fort Worth).	24
Figure 9. Relationship between erodibility index and particle diameter.	28
Figure 10. SSEA erosion results with no to light damage to the spillway (0.9% of the material was removed).	31
Figure 11. SSEA erosion results with moderate damage to the spillway (34.78% of the material was removed).	31
Figure 12. SSEA erosion results showing the spillway breached (77.78% of the material was removed).	32
Figure 13. Hypothetical (y,x) data scattered around the true regression line for n = 5 (modified after Walpole et al. 2002).	35
Figure 14. Probability of erosion by logistic regression of case histories (Wibowo and Murphy 2005).	38
Figure 15. Probability of erosion by logistic regression for Annandale's threshold line (Wibowo and Murphy 2005).	39
Figure 16. Tuttle Creek Spillway after being used during the Flood of 1993.	42

Tables

Table 1. Material strength number (M_s) for cohesionless soils (USDA 1997).	16
Table 2. Material strength number (M_s) for cohesive soils (USDA 1997).	17
Table 3. Material strength number (M_s) for rock (USDA 1997).	18
Table 4. Joint set number, J_n (USDA 1997).	19
Table 5. Joint roughness number, J_r (USDA 1997).	21
Table 6. Joint alteration number, J_a (USDA 1997).	21
Table 7. Relative ground structure number, J_s (USDA 1997).	23
Table 8. SSEA input interface parameters.	27

Table 9. Examples of erosion index values for some geologic materials..... 27

Table 10. Variables used for the parametric studies and their values.....30

Table 11. Probability of spillway damages using ordinal logistic regression. 41

Preface

The work described in this report was authorized by Headquarters, U.S. Army Corps of Engineers (HQUSACE), as part of the Flood and Coastal Storm Damage Reduction Research Program. The study was conducted and funded by two work units, "Breaching Mechanics for Embankment Dams," and "Unlined Spillway Erosion Risk Assessment," both managed at the U.S. Army Engineer and Research Development Center (ERDC), Vicksburg, MS.

This report summarizes work performed by Evelyn Villanueva and Dr. Johannes L. Wibowo of the Geotechnical Engineering and Geosciences Branch (GEGB), Geosciences and Structures Division (GSD), Geotechnical and Structures Laboratory (GSL), ERDC. The authors acknowledge the contributions of Dr. Mitchell L. Neilsen of Kansas State University and Darrel M. Temple of the U.S. Department of Agriculture, Agricultural Research Service. The study was conducted under the supervision of Dr. Monte L. Pearson, Chief, GEEB, and Dr. Robert L. Hall, Chief, GSD. Dr. William P. Grogan was Deputy Director, GSL, and Dr. David W. Pittman was Director, GSL.

COL Gary E. Johnston was Commander and Executive Director of ERDC. Dr. James R. Houston was Director.

1 Introduction

According to the World Register of Dams database (1998) maintained by the International Commission on Large Dams, over 60% of the dams currently in operation in the world are earthen dams, and, for this reason, a high number of open channel spillways are also operating.

The single most common cause of earthen dam failures is overtopping from an undersized spillway. Another cause of spillway breach and subsequent dam failure is extensive erosion of unlined spillways. Therefore, spillway design is critical to reservoirs. A spillway must have sufficient capacity to allow for the conveyance of peak flows during floods. Spillway design must also consider impact to human life and potential property damage. Further consideration must be given to the likelihood of downstream development that may elevate the hazard classification.

Advances in computer modeling have allowed the simplification of the complex spillway erosion prediction process in the Water Resources Site Analysis Program (SITES) developed by the United States Department of Agriculture (USDA), the Agricultural Research Service (USDA-ARS), the USDA Natural Resources Conservation Service (USDA-NRCS), and the Kansas State University. Through more in-depth research in conjunction with the U.S. Army Corps of Engineers (USACE), SITES was adapted to quantify the amount of damage. This new software was named SITES Spillway Erosion Analysis (SSEA). A recent revision of SITES emulates the response of the spillway by generating a distribution of reasonable collections of parameter values by adding the Latin Hypercube Sampling (SSEA+LHS) statistical method. This revision was not used for this research.

Spillway erosion is highly dependent on the variable nature of the channel geometry, geologic material, and uncertain flood discharge. Moore et al. (1994) define spillway performance by a threshold line, which divides erosion from nonerosion. To account for much uncertainty, the unlined spillway erosion threshold line was expanded for a range of probabilities into a series of threshold lines using multiple logistic regression. This initial binary assessment was then advanced using ordinal logistic regression on a spillway erosion database built on parametric studies to develop a prob-

abilistic model. The model was used to estimate the amount of erosion (quantitative) and then sorted into three qualitative levels of damage: (1) No to Slight Damage, (2) Moderate Damage, and (3) Severe Damage to Breach.

The basis for the development of the dataset was derived from studies of spillway erosion case histories by the USDA and USACE. This research is based on parameters found in previous research to be the leading factors influencing spillway damages due to flood discharge; channel geometry, which is described by the length and slope of the spillway channel; stream hydrology, specifically the maximum (peak) flood discharge and the duration of the flood; and the geologic material, expressed by a headcut erodibility index. For this study, a procedure was developed that compares the erosion damage level of 275 cases using the SSEA model with results obtained using ordinal logistic regression. To assess the procedure's reliability, it was also applied to case histories. The findings from this study can be part of a risk assessment tool that may be used for quick screening and decision-making.

2 Previous Studies

Erosion of an unlined auxiliary spillway is a complex process. The existing engineering guidance related to unlined spillway erosion provided by the USACE in 1994 was limited to the suggested permissible velocities for non-scouring channels. In 1990, the USACE stated that the designer must not only decide whether the channel materials will be eroded, but also make a reasonable estimate pertaining to the rate at which erosion will progress. Early design of vegetated earthen spillways by the USDA used an implied erosion rate by designating a bulk length through the crest that varied with the material and the total outflow per unit of spillway width (USDA, SCS 1973). Experience with these spillways was combined with laboratory studies of the underlying erosion processes to develop a model to predict the breach potential of vegetated earthen spillways that was then incorporated into the SITES design/analysis software used by USDA (USDA, NRCS 1996). The analysis of unlined spillway erosion involves three main groups of parameters:

1. Hydrodynamic power that causes erosion.
2. Geologic material properties that resist erosion.
3. Geometry of spillway.

In general, spillway erosion analysis is an empirical engineering procedure based on the correlation between the above parameters. The Repair, Evaluation, Maintenance, and Rehabilitation (REMR) rapid evaluation, conducted by the USACE Waterways Experiment Station (WES), relies on hydrodynamic and geologic material properties. Work by Annandale (1995) addresses the previously mentioned parameters 1 through 3. The USDA model includes hydrodynamic factors, geologic material properties, and the geometry. This chapter summarizes the USDA model and discusses its application using the SSEA computer program. This study uses the SSEA (v. 2005) program to predict unlined spillway channel erosion.

In addition to the ongoing efforts of the USDA, research conducted by Bollaert and Schleiss (2002) attempts to combine all these parameters in the evaluation of plunge pool erosion. In this study, they evaluate the scour depth due to high velocity jet impact. Ongoing research is continuing

to advance the technology in this area, and refinements may be expected as knowledge increases.

USDA model

In 1983, the Soil Conservation Service (SCS) of the USDA organized the Emergency Spillway Flow Study Task Group (ESFSTG) to collect information from vegetated earthen spillways that had experienced significant hydraulic attack or erosion. This effort compiled data from more than 80 sites representing 13 flood events in 10 states over the period of 8 years. During the same period, the research arm of the USDA, the Agricultural Research Service, carried out research on underlying erosion processes related to spillway performance.

The USDA researchers found that the erosion of earthen spillways, as observed in the field and laboratory, could be divided into the following three sequential phases: failure of vegetal cover (Phase 1), development of vertical headcut (Phase 2), and advancement of headcut (Phase 3), as shown in Figure 1.

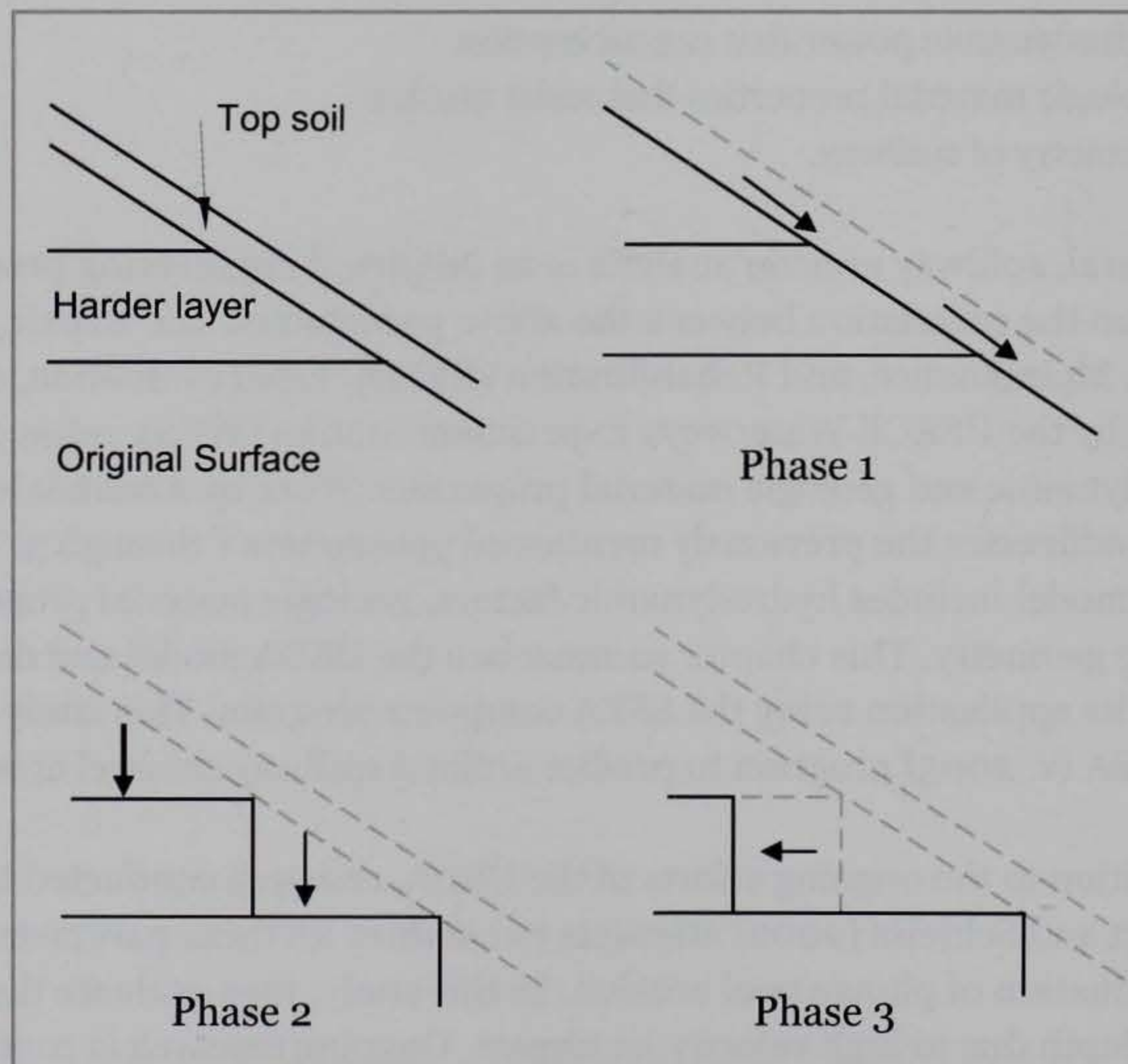


Figure 1. The three phases of headcut erosion (after USSD 2004).

The first two phases are modeled with shear stress concepts, and the third phase makes use of the energy dissipation rate. Each of the phases is described in separate threshold-rate relations. A brief overview of all three phases is discussed herein. The model is two-dimensional in the sense that erosion width is not tracked, but the effects of flow concentration are accounted for to a limited extent in development of the governing relationships.

Phases 1 and 2 of the erosion processes (Temple and Hanson 1993) are simulated with a detachment rate model in which the erosion rate is proportional to the excess erosionally effective stress, τ_e , above a critical shear stress value, τ_c .

Phase 1 consists of erosion of soil through the vegetal cover leading to cover failure. The erosionally effective stress is the stress on the soil particles contained within the soil and vegetal root matrix. It is computed by partitioning the traction stress using a relation incorporating a vegetal cover factor, the soil grain roughness of the underlying soil expressed in terms of Manning's coefficient, and the Manning's n of the channel as a whole. Manning's roughness coefficient values are used in Manning's formula for flow calculation in open flow channels. The cover factor can be used to account for the quality of the cover and the presence of discontinuities that might concentrate stresses. Under the assumption that the erosionally effective stress $\tau_e \gg \tau_c$ for soils is able to support meaningful vegetal cover, the critical shear stress is assumed to be zero in Phase 1, and the erosionally effective stress is integrated through time until the integral reaches a value associated with failure of the vegetal cover. This threshold is related to the plasticity index of the soil.

In Phase 2, the erosion continues into the material below the vegetal cover. In this phase, the critical shear stress is determined from Shields' criteria as shown in Figure 2 (USDA, NRCS 1997). The detachment rate coefficient is determined from a relation based on regression analysis of 10 documented studies of 98 fine-grained materials. The relation incorporates the dry unit weight and percent clay of the soil material. Alternatively, the coefficient may be determined from a direct measurement of soil erodibility using a jet index test described by Hanson (1991). As Phase 2 erosion continues, a vertical drop begins to form. The erosion in Phase 2 continues until the depth of the drop is equal to critical depth, at which point the

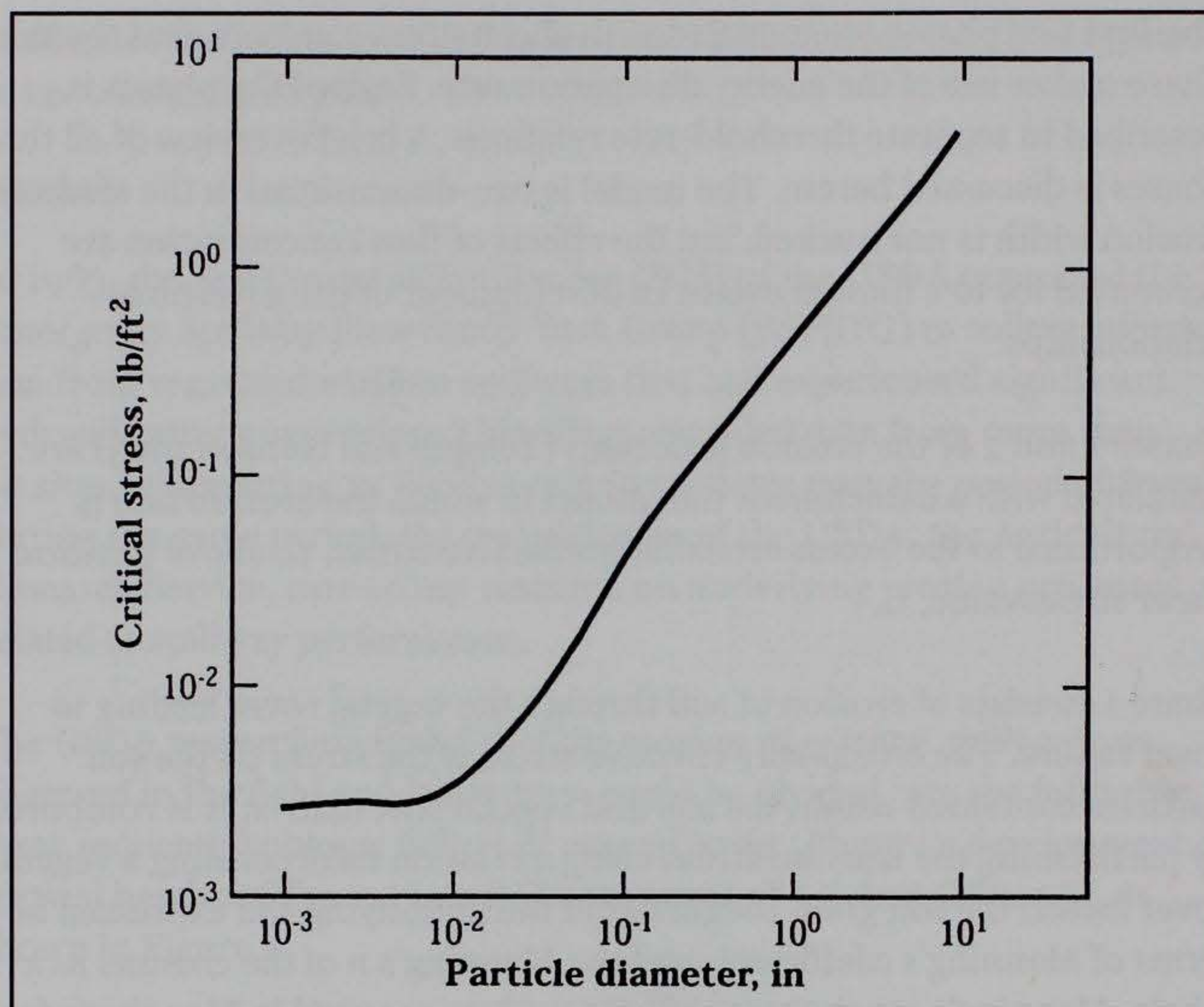


Figure 2. Critical stress for incipient motion calculated from Shield's criteria used in Phase 2 (USDA, NRCS 1997).

drop is judged sufficient to cause significant concentration of stress and flow energy dissipation at the base of the overfall.

Phase 3 erosion consists of the upstream advance of the headcut (Moore et al. 1994, Temple and Moore 1994). The model uses a threshold-rate relation for prediction of headcut advance with the material resistance dependent on the headcut erodibility index and the hydraulic attack expressed in terms of energy dissipation rate (stream power).

Erosion models threshold line

In the USDA and Annandale (Annandale 1995) models, the relation between stream power and erodibility index led to the development of a threshold line between erosion and nonerosion. Figure 3 shows schematically the threshold line concept. The horizontal axis in the erodibility index represents the resistance of geologic material against erosion, and the vertical axis represents the stream power. The threshold line defines a limit, below which the material will not erode. Annandale (1995) calculates

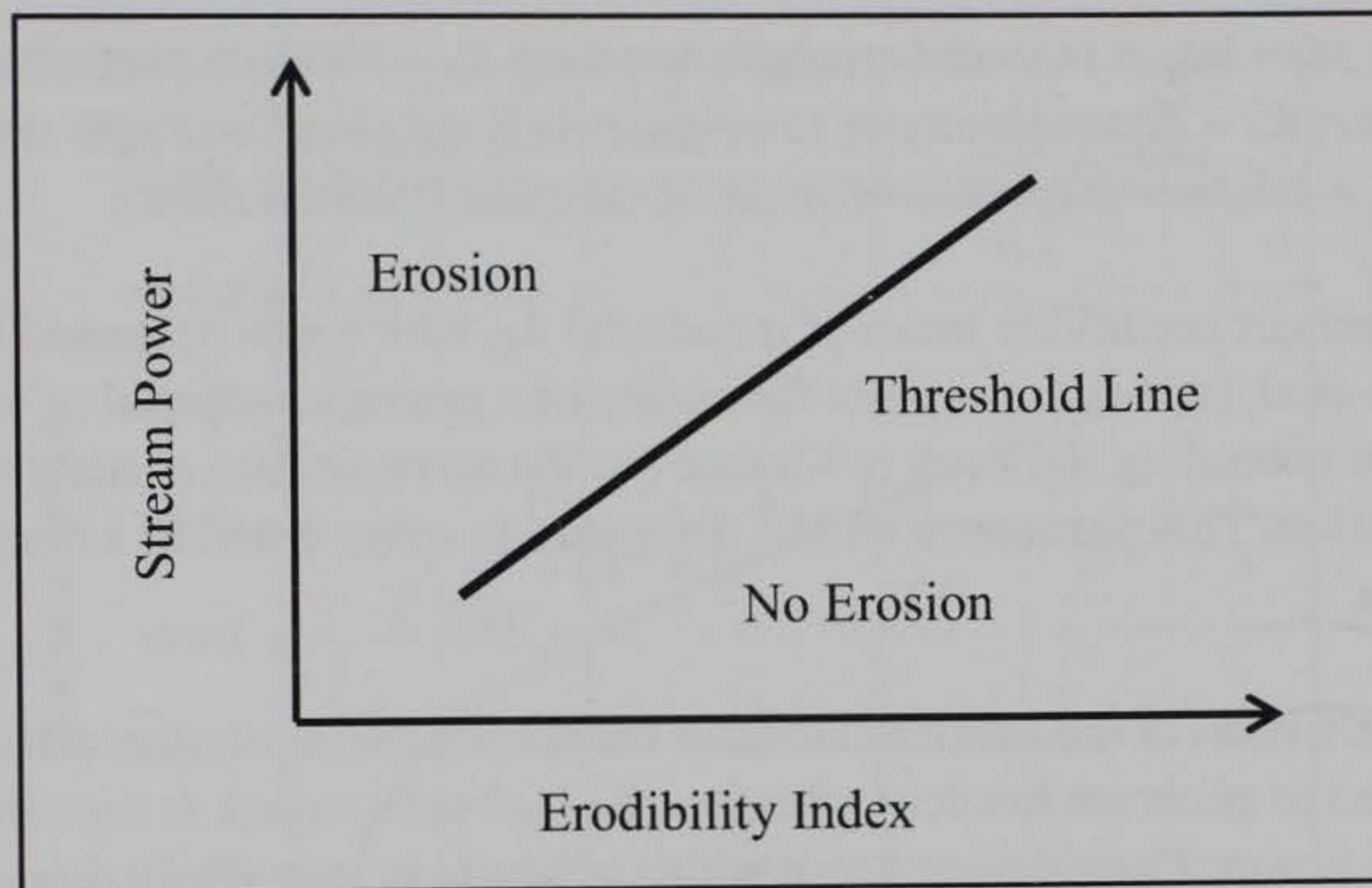


Figure 3. Sketch of threshold line concept showing stream power versus erodibility index (Wibowo et al. 2005).

the stream power rigorously while the USDA uses a simplified concept. Stream power per unit area is expressed as:

$$P = \gamma q S_f \quad (1)$$

where

- γ = unit weight of water
- q = unit discharge
- S_f = energy slope

The USDA simplified stream power by directly relating energy slope to the spillway slope which is applicable to the case of long spillway channel flows:

$$P = q H \quad (2)$$

where H is the height of the spillway drop.

Both Annandale (1995) and the USDA use the erodibility index which was derived from the excavatability index (Kirsten 1982) without significant modification:

$$K = M_s \cdot K_b \cdot K_d \cdot J_s \quad (3)$$

where M_s = intact material strength number; K_b = block or particle size number; K_d = discontinuity or inter-particle bond shear strength number; and J_s = relative shape and orientation number (Kirsten 1982).

The headcut erodibility index of a material K_h , which was proposed by Moore et al. (1994), represents the ability of a geologic material to resist erosion extending the work of Kirsten (1988) on resistance of material to excavation. This parameter will be discussed in more detail in a next section.

For evaluation of the headcut advance threshold, the minimum attack required to generate headcut advance, the hydraulic attack is expressed as stream power. Considering a unit width of headcut, the energy dissipated by the flow per unit of time (stream power) by flow over the headcut is given by:

$$E = q * \gamma * H \quad (4)$$

where

q = volume of flow over the headcut per unit of width

γ = unit weight of water

H = drop of the energy grade line as flow passes over the headcut

Figure 4 shows the correlations between the energy dissipation rate and the erodibility index for thresholds that were developed using data collected from spillway headcuts observed in the field by the USDA ARS.

The Phase 3 involves the headcut advance rate prediction. It was derived based on the energy dissipation rate (power) in excess of the threshold, using the relation:

$$\frac{dX}{dt} = \begin{cases} C(A - A_0) & A \geq A_0 \\ 0 & A < A_0 \end{cases} \quad (5)$$

with

$$A = (qH)^{1/3} \quad (6)$$

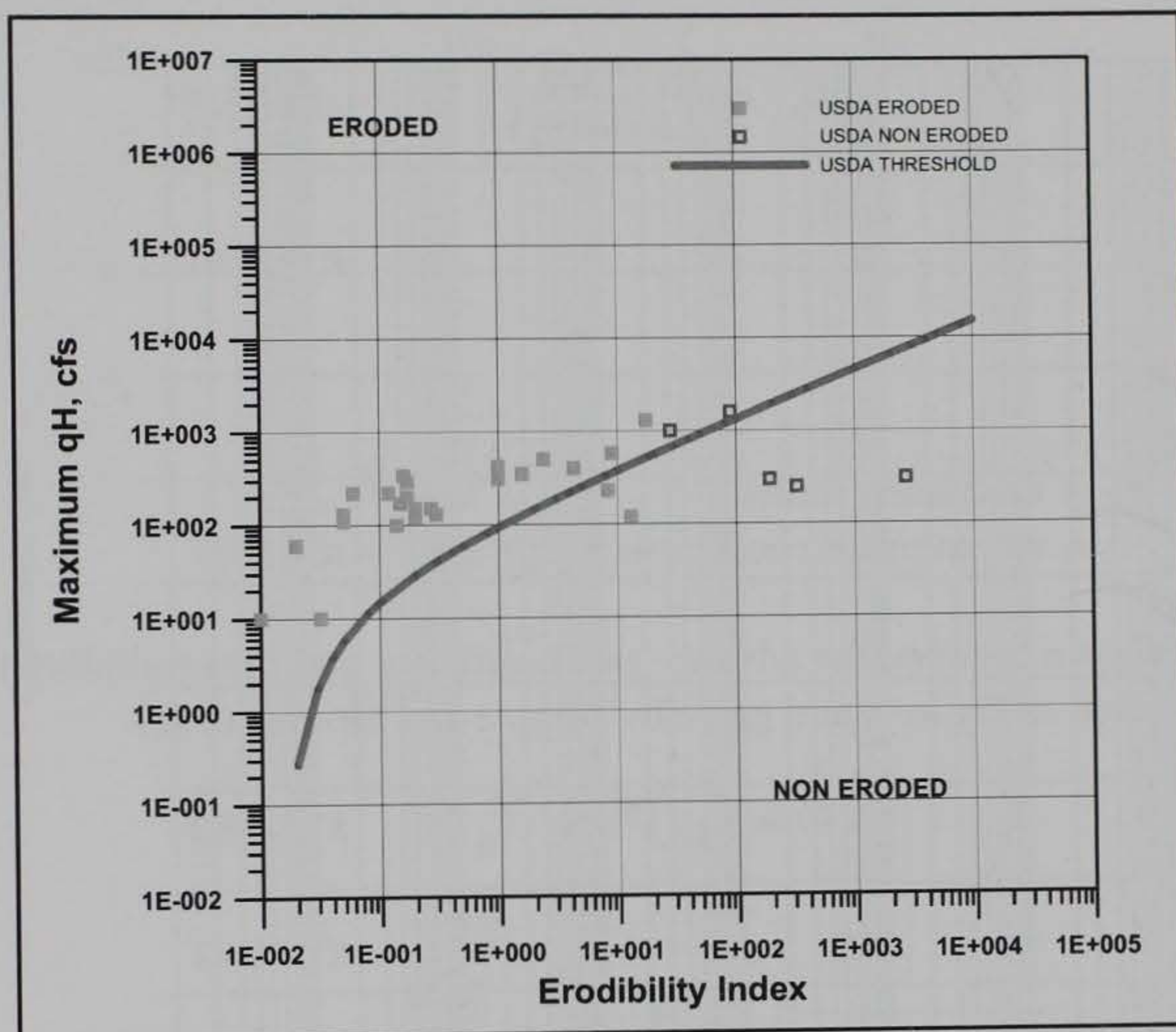


Figure 4. Threshold line developed by USDA (Moore et al. 1994).

where

$\frac{dX}{dt}$ = advance rate of the headcut (positive upstream)

C = advance rate coefficient

A = applied hydraulic attack

A_o = advance threshold defined as the level of attack below which no advance occurs

q = unit discharge in the spillway

H = height of the headcut

The power term in Figure 3 and Equation 6 has been simplified to qH to reflect only the independent variables in Equation 4. It is generally necessary to simplify application of the approach further by assuming that the drop in the energy grade line is equal to the height of the overfall.

The relation of advance rate coefficient and advance threshold to the erodibility index was developed from ESFSTG data as described by Moore et al. (1994) and Temple and Moore (1994). The advance threshold is given by:

$$A_0 = \begin{cases} \left[a K_h^{1/2} \exp\left(\frac{-3.23}{\ln(101K_h)}\right) \right]^{1/3} & K_h \geq 0.01 \\ 0 & K_h < 0.01 \end{cases} \quad (7)$$

where

K_h = erodibility index

a = an empirical coefficient = 5.35 m³/s = 189 ft³/s

The relation between the advance rate coefficient and the erodibility index is depicted in Figure 5 and given by Temple and Moore (1994):

$$C = \begin{cases} -0.79 \ln(K_h) + 3.04 & K_h \leq 18.2 \\ 0.75 & K_h > 18.2 \end{cases} \quad (8)$$

The headcut advance coefficient C is expressed in (m/h)/(m³/s)^{1/3} or (ft/h)/(ft³/s)^{1/3}. Equation 8 was developed for relatively weak materials. The bottom half of Equation 8 (where K_h values are greater than 18.2) is a bound of the relation rather than a fit of data in that region.

The model was applied to predict the potential for breach of spillways of the type used by USDA on watershed flood control reservoirs. Because different phases may dominate the process for different conditions, the model is applied iteratively to different erosion scenarios to determine which scenario represents the greatest potential to generate a breach. The points of headcut initiation that are evaluated include the location of each change in slope, surface, or cover condition in the spillway plus additional locations that are identified as potentially exposing erodible subsurface materials most rapidly. As the headcut progresses through multiple materials, the advance rate of secondary headcuts following material interfaces is examined in addition to evaluating the advance rate of the headcut that continues deepening in accordance with the stress-based detachment rate relation. As previously noted, this is a first generation of a semi-empirical computational model, and it was originally implemented in the SITES software. The model is two-dimensional in the sense that only the downward and upstream advance of the erosion are evaluated, and the energy that drives the headcut deepening and advance is based on the discharge

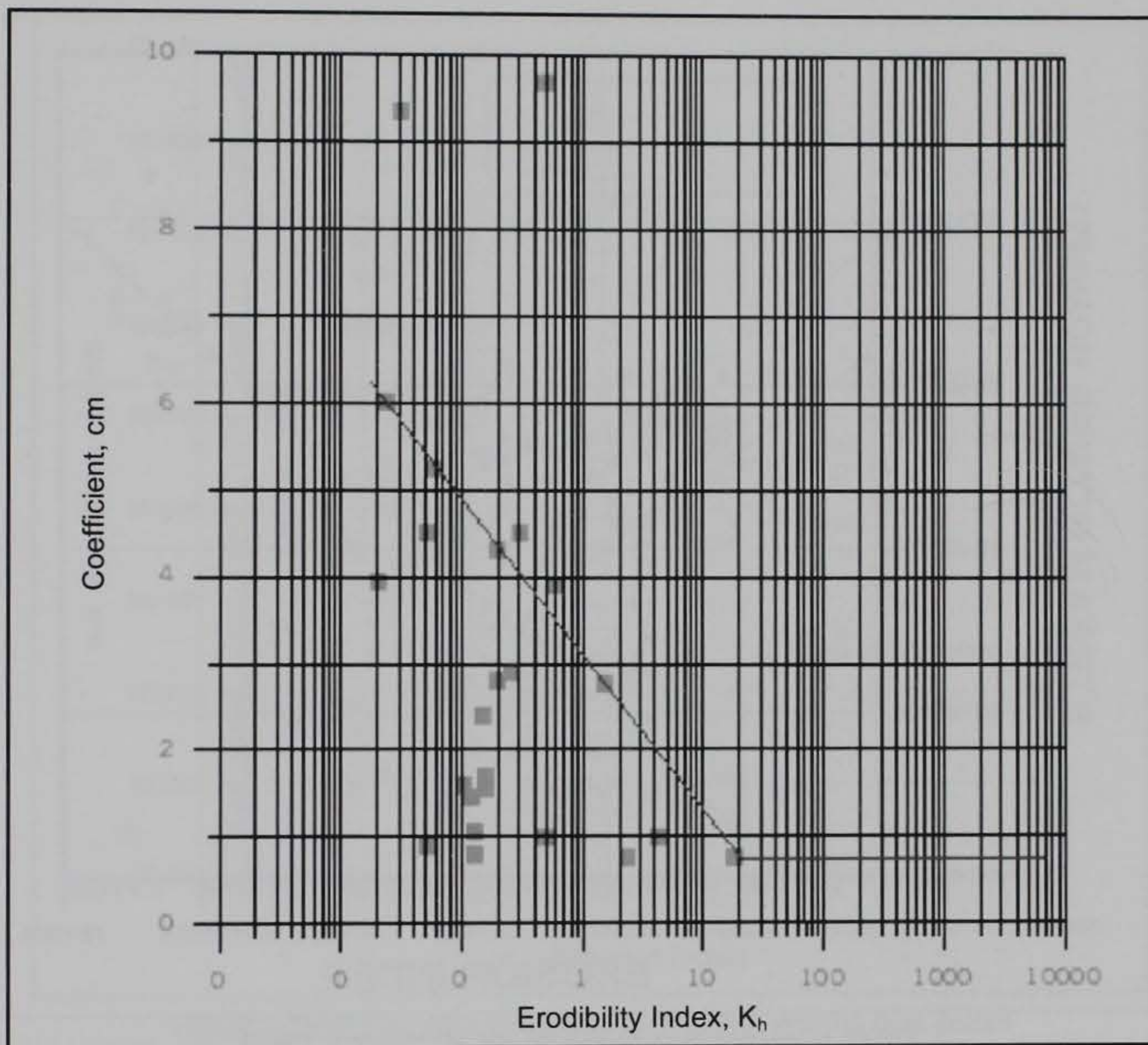


Figure 5. Curve for determination of headcut advance rate coefficient (Temple and Moore 1994).

per unit width. Because the model is first generation and semi-empirical, it is expected that the governing relations will be refined as more data becomes available and more studies are conducted. Particularly lacking in the original USDA dataset used in the model development were data from spillways with large discharges that generate damage in erosion resistant materials.

The Annandale erosion threshold line, which is shown in Figure 6, is more generic and can be applied directly to evaluate spillway stability. However, the USDA threshold line was developed specifically for headcut erosion cases. The application of this threshold line, as well as the Latin Hypercube Sampling capability, has been incorporated into the upgraded SSEA model. Figure 7, in the following section, shows the USDA threshold line with additional data points from recent USACE spillway erosion case histories.

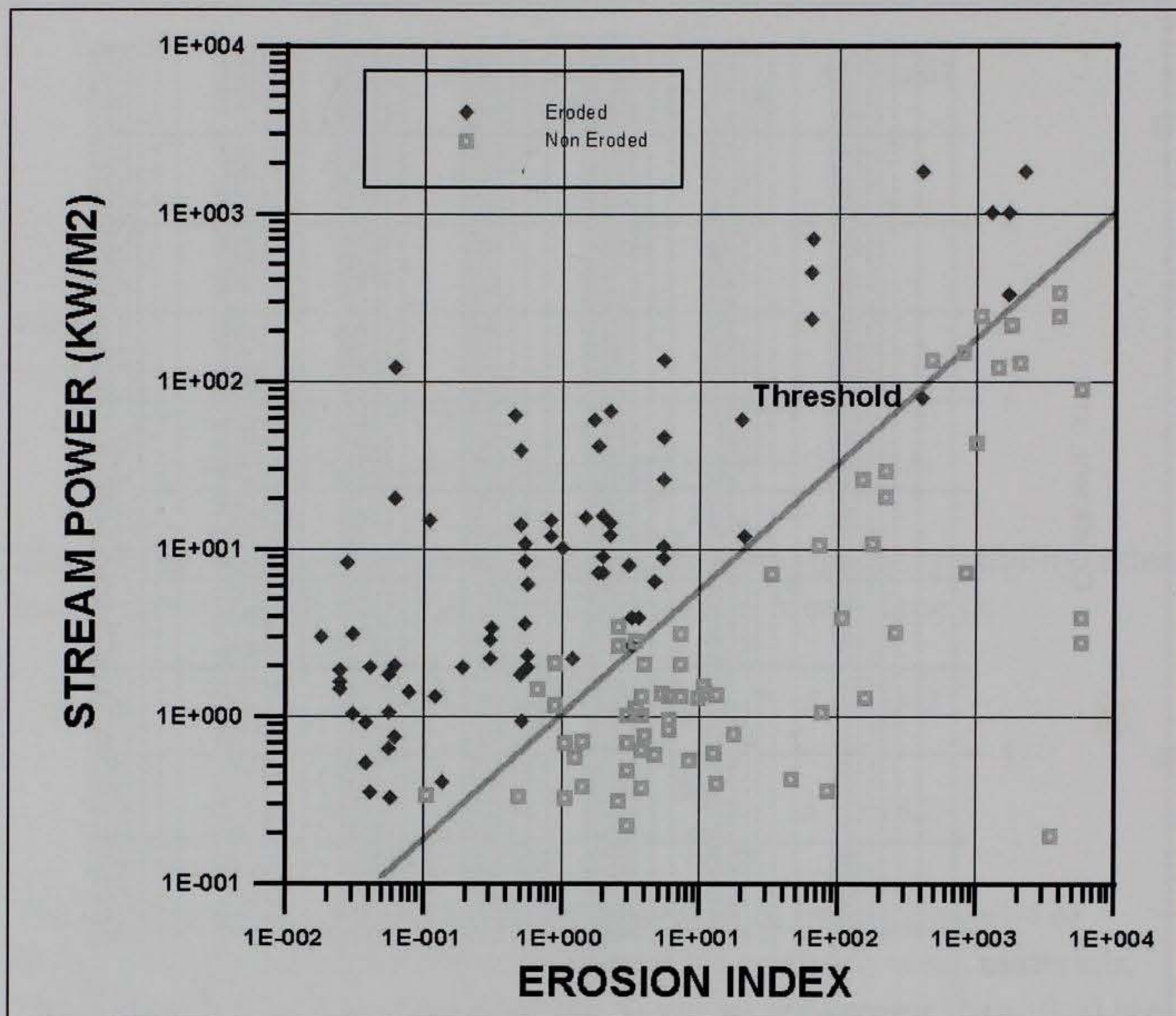


Figure 6. Annandale's threshold line (Annandale 1995).

Threshold zone

Additional erosion data was collected from Tuttle Creek Spillway, Kansas, and Saylorville Spillway, Iowa, among others, and provided by the USACE Kansas City District (KCD) and the Rock Island District (RID), respectively. When plotting the approximately 100 additional erosion data points from case histories, it was found that some erosion data points fell below the erosion threshold line as shown in Figure 7. It demonstrates that there is no distinct boundary which we attribute to the uncertainty in the variability of geologic material, complicated flow behavior, and modeling assumptions. In an unpublished report, Wibowo and Murphy concluded in 2005 that the threshold region is not a well-defined linear single line, but is more like a threshold zone. Therefore, for a data point that falls within the zone, there is an uncertainty whether the material will erode or not. This finding leads to the applicability of using logistic regression in developing a family of threshold lines.

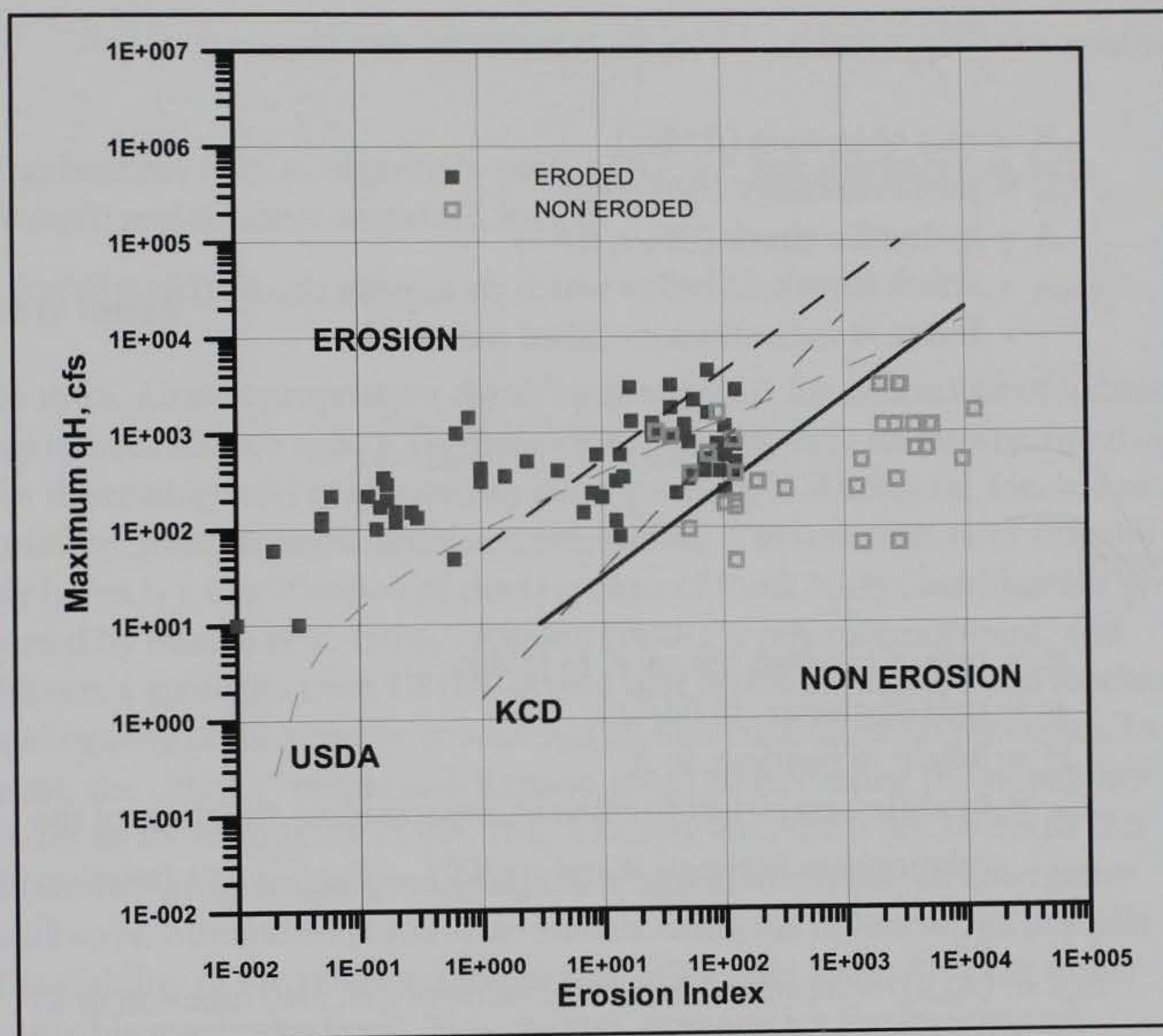


Figure 7. Threshold zone developed from USACE erosion data points (Wibowo and Murphy 2005).

To produce a conservative analysis, the threshold line is translated to the right side to cover all eroded data points. This new line, however, envelops some non-eroded points as well. A lower threshold line, below which only non-erosion data exist, is then established. This complements the upper bound threshold line, above which only erosion data points exist, leaving a transition area between these two boundaries of mixed cases. There are uncertainties that are inherent in this erosion model which come from the natural variability of materials and/or from the methodology itself. For a conservative prediction of erosion, it is recommended that the lower bound threshold line be used. The transitional zone between the upper and lower bound thresholds provides a measure of uncertainty in erosion prediction and triggered studies in spillway erosion risk assessment. To predict headcut erosion, a similar basic equation, as used by USDA and KCD in 2004, is applied in this model's formulation:

$$R = C_m [A - A_{o,m}] \quad (9)$$

where

- R = rate of erosion (ft/day)
- C_m = proportionality coefficient
- A = hydraulic attack ((ft³/s/ft)^{1/3})
- $A_{o,m}$ = attack threshold below which no erosion occurs ((ft³/s/ft)^{1/3})
- Index m indicates a modified parameter

$$R = C_m \left[(qH)^{1/3} - (E_{t,m})^{1/3} \right] \quad (10)$$

where

- R = rate of headcut advance, in ft/day
- q = unit discharge, in ft³/s/ft
- H = height of headcut, in ft
- C_m = modified empirical coefficient, representing the slope of the relationship between R and $\left[(qH)^{1/3} - (E_{t,m})^{1/3} \right]$ as a function of K_h
- $E_{t,m} = (A_{o,m})^3$ = modified threshold value of qH , also function of K_h
- K_h = headcut erosion index

The proposed lower bound threshold line is:

$$(A_o)^3 = 3.57 (K_h)^{0.937} \quad (11)$$

The coefficient C_m is expressed as

$$C_m = \frac{R}{\left[(qH)^{1/3} - \left(3.57 (K_h)^{0.937} \right)^{1/3} \right]} \quad (12)$$

Using regression analysis on the data from USDA and USACE case histories, Equation 12 can be expressed as

$$C_m = \exp \left[2.455 - 0.707 \ln (K_h) \right] \quad (13)$$

The new expression of rate of erosion is:

$$R = \exp[2.455 - 0.707 \ln(K_h)] [(qH)^{1/3} - 0.361(K_h)^{4/9}] \quad (14)$$

The headcut rate, R , is given in units of ft/day; unit discharge, q , is in ft³/s/ft; and headcut height, H , is in ft.

Erodibility index

In 1982, Kirsten proposed a classification system for excavation of natural materials (Kirsten 1982). The index uses four geologic material properties for describing level of excavation efforts: strength of material, block size number, joint strength, and joint orientation. This excavation or rippability index is a modification of the Q system of Rock Mass Classification proposed by Barton et al. (1974). Kirsten (1988), a private consultant, and Moore, a geologist from USDA, agreed that hydraulic erosion and mechanical ripping of rock can be considered similar comminution processes. In 1991, the USDA (Temple and Hanson 1993) started using the rippability index as the erodibility index. They incorporated the index in the SITES computer program for predicting the progress of erosion on emergency spillways. Annandale (1992) also started using the index during analysis of the stability of the spillway plunge pool of Bartlett Dam, Arizona, under probable maximum flood. This chapter summarizes the history and characteristics of the erodibility index as used in erosion analysis.

The general form of the erodibility index (K_h) is:

$$K_h = M_s * K_b * K_d * J_s \quad (15)$$

where

- M_s = material strength number
- K_b = block or particle size number
- K_d = discontinuity or inter-particle bond shear strength number
- J_s = relative ground structure number

Material strength number (M_s)

The term M_s represents the strength of an intact material without considering the variability within the mass and is related to the unconfined compressive strength (UCS). Earth material may be categorized into three groups for estimation of the material strength number used in

determining the headcut erodibility index: cohesionless soil, cohesive soil, and rock. The value of material strength index can be determined using field identification tests, standard field tests, and/or laboratory tests appropriate for each of these material types.

Material strength number of cohesionless soil

The material strength number for cohesionless soil can be determined using relative density, field identification tests, Standard Penetration Test (SPT), or the In-situ Deformation Modulus (IDM). The relation of the IDM M_s is given by:

$$M_s = 1.7(IDM)^{0.832} \quad (16)$$

with IDM in MPa. The IDM is determined using ASTM D-1194. This test provides the IDM of material up to a depth equal to about two diameters of the bearing plate (the maximum-diameter bearing plate is 30 in.). If cohesionless material is found at a depth of more than 5 ft, M_s can be determined using the SPT (ASTM D-1586). The material strength number for cohesionless soils is given in Table 1.

Table 1. Material strength number (M_s) for cohesionless soils (USDA 1997).

Relative Density	Field Identification Tests	SPT (blows/0.3)	In-situ deformation modulus (IDM) (MPa)	M_s
Very loose	Particles loosely packed. High percentage of voids. Very easily dislodged by hand. Matrix crumbles easily when scraped with point of geologic pick. Raveling often occurs on excavated faces.	<5	<0.005	< 0.02
Loose	Particles loosely packed. Some resistance to being dislodged by hand. Large number of voids. Matrix shows low resistance to penetration by point of geologic pick.	5-10	0.005-0.01	0.02-0.05
Medium dense	Particles closely packed. Difficult to dislodge individual particles by hand. Voids less apparent. Matrix has considerable resistance to penetration by point of geologic pick.	10-30	0.01-0.03	0.05-0.10
Dense	Particles very closely packed and occasionally very weakly cemented. Cannot dislodge individual particles by hand. The mass has very high resistance to penetration by point of geologic pick. Requires many blows of geologic pick to dislodge particles.	30-50	0.03-0.08	0.10-0.20
Very dense	Particles very densely packed and usually cemented together. Mass has high resistance to repeated blows of geologic pick. Requires power tools for excavation.	>50	0.08-0.2	0.20-0.45

Material strength number of cohesive soil

The material strength number for cohesive soil can be determined using consistency, field identification tests, SPT, and UCS. The UCS can be determined using the Uniaxial Compression Test (ASTM D-2166), vane shear strength (ASTM D-2573) field test, or ASTM D-4648, laboratory test. For most cohesive soil, M_s can be determined using the following relation:

$$\begin{aligned} M_s &= 0.78(UCS)^{1.09} && \text{for } UCS \leq 10 \text{ MPa} \\ M_s &= UCS && \text{for } UCS > 10 \text{ MPa} \end{aligned} \quad (17)$$

The material strength numbers given in Table 2 represent rounded off products of uniaxial compressive strength and relative density coefficients.

Table 2. Material strength number (M_s) for cohesive soils (USDA 1997).

Consistency	Field Identification Tests	SPT (blows/0.3)	Unconfined Compressive Strength (UCS) (kPa)	M_s
Very soft	Exudes between fingers when squeezed in hand.	<2	<40	<0.02
Soft	Easily molded with fingers. Point of geologic pick easily pushed into shaft of handle.	2-4	40-80	0.02-0.05
Firm	Penetrated several centimeters by thumb with moderate pressures. Molded by fingers with some pressure.	4-8	80-150	0.05-0.10
Stiff	Indented by thumb with great effort. Point of geologic pick can be pushed in up to 1 centimeter. Very difficult to mold with fingers. Just penetrated with hand spade.	8-15	150-300	0.10-0.20
Very stiff	Indented only by thumbnail. Slight indentation by pushing point of geologic pick. Requires hand pick for excavation.	15-30	300-625	0.20-0.45

Material strength number of rock

The material strength number of rock can be determined using rock hardness, field identification tests, or UCS. The UCS can be determined using ASTM D-2938 or the Point Load Test (ASTM D-5731). For most rock, M_s can be determined using Equation 17. The material strength number for

rock is given in Table 3. Hardness categories are based on hardness characteristics and not on geological origin.

Block/particle size number

The second component of the erodibility index is K_b , which is the average size of the individual material block unit estimated by the spacing of discontinuities in rock masses or by average particle diameter (D_{50}) of cohesionless granular soil.

Table 3. Material strength number (M_s) for rock (USDA 1997).

Rock Material Hardness	Uniaxial Compressive Strength (MPa)	Field Identification Tests	M_s
Very soft rock or hard, soil-like material	0.6-1.25	Scratched with fingernail. Slight indentation produced by light blow of point of geologic pick. Requires power tools for excavation. Peels with pocket knife.	0.45-1.0
Soft rock	1.25-5.0	Hand-held specimen crumbles under firm blows with point of geologic pick.	1.0-4.5
Moderately soft rock	5.0-12.5	Shallow indentations (1 to 3 mm) produced by light blows with point of geologic pick. Peels with pocket knife with difficulty.	4.5-12.5
Moderately hard rock	12.5-50.0	Cannot be scraped or peeled with pocket knife. Intact hand-held specimen breaks with single blow of geologic hammer. Can be distinctly scratched with 20d common steel nail.	12.5-50.
Hard rock	50.0-100.0	Intact hand-held specimen requires more than one hammer blow to break it. Can be faintly scratched with 20d common steel nail.	50-100
Very hard rock	100.0-250.0	Intact specimen breaks only by repeated, heavy blows with geologic hammer. Cannot be scratched with 20d common steel nail.	100-250
Extremely hard rock	>250.0	Intact specimen can only be chipped, not broken, by repeated, heavy blows of geologic hammer.	>250

The value of K_b for rock and rock-like material is estimated using the following relation:

$$K_b = \frac{RQD}{J_n} \quad (18)$$

where

RQD = Rock Quality Designation

J_n = joint set number

The Rock Quality Designation (*RQD*) was originally introduced by Deere (1964) to express the behavior of rock mass for tunneling purposes (Deere and Deere 1988). The *RQD* is a modified core recovery that discounts small core fragments and lost core. By definition, the *RQD* is defined as the sum of the length of core pieces greater than 4 in. divided by the total length of sampled core run, as a percentage. Barton et al. (1974) found that the relation of span width and *RQD* could be improved if the *RQD* value is divided by a number related to the number of joint sets. The original number of joint sets proposed by Barton et al. (1974) ranged between 0.5 for massive rock and 20 for crushed rock. Kirsten (1982) modified this J_n number to a range of 1.0 to 5.0, as shown in Table 4.

Table 4. Joint set number, J_n (USDA 1997).

Joint Set	Joint Set Number, J_n
Intact, no or few joints	1.00
One joint set	1.22
One joint set plus random	1.50
Two joint sets	1.83
Two joint sets plus random	2.24
Three joint sets	2.73
Three joint sets plus random	3.34
Four joint sets	4.09
More than four joint sets	5.00

There are several ways to calculate *RQD* depending on the kind of information available for the rock mass. For a rock mass described by the number of joints per cubic meter, the following relation can be used:

$$RQD = (115 - 3.3J_c) \quad (19)$$

where J_c = joint count number representing the number of joints per cubic meter.

For a rock mass describing the number of joints in three Cartesian axes, *RQD* can be determined using the formula:

$$RQD = \left(105 - \frac{10}{D} \right) \quad (20)$$

where

$$D = (J_x * J_y * J_z)^{1/3}$$

J_x = number of joints in the direction perpendicular to flow

J_y = number of joints in the direction of flow

J_z = number of joints in vertical direction

For intact cohesive material, the value of $K_b = 1$. For cohesionless granular material, Kirsten (after Annandale 1995) suggested that

$$K_b = 1000 D_{50}^3 \quad (21)$$

Discontinuity bond shear strength number

The discontinuity bond shear strength number K_d is expressed as the ratio:

$$K_d = \frac{J_r}{J_a} \quad (22)$$

where

J_r = joint roughness number

J_a = joint alteration number

The joint roughness number represents the degree of roughness of joint surfaces. Table 5 shows that the value of joint roughness, J_r , ranges from 0.5 for a slickensided, planar joint to 4.0 for discontinuous or stepped joints. Joint alteration number describes the level of alteration of the joint walls or filling material. Kirsten (1982) simplified Barton's chart, but the value is similar. Table 6 shows values of J_a ranging from 0.75 for a tightly healed joint to 18.0 for a joint with an aperture >5.0 mm with a swelling clay filling. Barton et al. (1974) found that the $\tan^{-1}(J_r/J_a)$ is a fair approximation of the actual shear strength.

Table 5. Joint roughness number, J_r (USDA 1997).

Joint Separation	Joint Roughness Condition	J_r
Joints are tight or become closed during hydraulic flow	Discontinuous joints; stepped	4.0
	Rough/irregular: undulating (e.g., tension joints, rough sheeting joints, rough bedding)	3.0
	Smooth; undulating (e.g., smooth sheeting, nonplanar foliation and bedding)	2.0
	Slickensided; undulating	1.5
	Rough/irregular; planar	1.5
	Smooth; planar (e.g., planar sheeting joints, planar foliation and bedding)	1.0
	Slickensided; planar	0.5
Joints are open and remain open during hydraulic flow	Joints are either open or contain relatively soft gouge of sufficient thickness to prevent wall contact during hydraulic flow	1.0
	Joints contain swelling clays	1.0

Table 6. Joint alteration number, J_a (USDA 1997).

Field Identification of Gouge (Infilling)	J_a for Aperture Width, mm		
	<1.0	1.0-5.0	>5.0
Joint tightly healed with hard, nonsoftening, impermeable mineral filling, e.g., quartz, calcite, or epidote.	0.75	1.0	1.5
Clean, open joint with fresh or discolored (unweathered) walls only; no infilling.	1.0	1.5	2.0
Discolored to disintegrated joint walls; infilling is sand or gravel with <15% cohesionless fines in matrix; with or without disintegrated or crushed rock fragments.	2.0	4.0	6.0
Discolored to disintegrated joint walls; cohesionless, nonswelling, low to nonplastic: fines in matrix; with or without disintegrated or crushed rock fragments.	3.0	6.0	10.0
Disintegrated to decomposed joint walls; nonswelling, lean clay or clay matrix, or low friction clays, such as chlorite, talc, mica, serpentine, gypsum, graphite, kaolinite, or other sheet silicates; with or without disintegrated or crushed rock fragments.	4.0	8.0	13.0
Disintegrated to decomposed joint walls; fat clay, swelling clay, such as montmorillonite, or clay matrix, with or without disintegrated or crushed rock fragments.	5.0	10.0	18.0

Relative ground structure number

The relative orientation of ground structure and the joint spacing contributes to the kinematics of dislodgement of individual blocks. The final formulation of the relative ground structure number depends on apparent dip, ratio of joint spacing, and flow direction. The ratio of joint spacing is defined as the ratio of the shortest side of a rectangular block of rock

(longitudinal section in direction of flow) to the longest side. The apparent dip can be calculated using the equation:

$$\tan a = (\tan b)(\sin c) \quad (23)$$

where

a = apparent dip of the discontinuity

b = true dip of the discontinuity

c = (strike of discontinuity) - (spillway flow direction)

For a spillway flow in the same direction as the apparent dip, the effective dip can be calculated using:

$$q = a - \alpha \quad (24)$$

where

q = effective dip

α = slope of spillway channel

For a spillway flow in the opposite direction of the apparent dip, the effective dip can be calculated using:

$$q = a + \alpha \quad (25)$$

The relative ground structure numbers are tabulated in Table 7. There are two categories of joint sets identified in the table: the first is the weaker joint set with dip direction with the flow direction, and the second is the weaker joint set with dip direction against the flow direction. Parameter r in Table 7 is the relative block shape defined as the ratio of joint spacing. A more detailed description on the erodibility index can be found in Kirsten (1982), Annandale (1995, 2002), USDA NRCS (1997), and Wibowo and Murphy (2005).

Table 7. Relative ground structure number, J_s (USDA 1997).

		r				
	q	1:1	1:2	1:4	1:8	
With flow	180/0	90	1.00	1.00	1.00	1.00
	0	85	0.72	0.67	0.62	0.56
	0	80	0.63	0.57	0.50	0.45
	0	70	0.52	0.45	0.41	0.38
	0	60	0.49	0.44	0.41	0.37
	0	50	0.49	0.46	0.43	0.40
	0	40	0.53	0.49	0.46	0.44
	0	30	0.63	0.59	0.55	0.53
	0	20	0.84	0.77	0.71	0.68
	0	10	1.22	1.10	0.99	0.93
	0	5	1.33	1.20	1.09	1.03
	0/180	0	1.00	1.00	1.00	1.00
	Against flow	180	5	0.72	0.81	0.86
180		10	0.63	0.70	0.76	0.81
180		20	0.52	0.57	0.63	0.67
180		30	0.49	0.53	0.57	0.59
180		40	0.49	0.52	0.54	0.56
180		50	0.53	0.56	0.58	0.60
180		60	0.63	0.67	0.71	0.73
180		70	0.84	0.91	0.97	1.01
180		80	1.22	1.32	1.40	1.46
180		85	1.33	1.39	1.45	1.50
180/0		90	1.00	1.00	1.00	1.00

Note: For granular material, $J_s = 1.00$. For values of r less than 1:8, take J_s as for $r = 1:8$.

3 Problem Statement

Significant advances in meteorology and flood hydrology have updated the maximum probable flood and design flood standards on which most of the existing dams were based. As a result, many dams may have insufficient spillway capacity. The response to high-level spillway flow includes channel floor and bank erosion, sediment transport and deposition, and overbank flooding. Erosion of the geologic material underlying unlined channels is the most serious of spillway flow impacts, because channel floor degradation can undermine spillway structures and threaten reservoir integrity. Figure 8 shows damage to Canyon Lake Spillway in Texas after a flood in July 2002. However, responses to spillway flow are not limited to the immediate area of the dam. Spillway overflow can cause stream thresholds to be exceeded in the main channels into which spillway flow exits. This overflow can influence or induce changes for significant distances downstream. The deposition of sediment coming from this flow can build bars and deltas in spillway channels, at the exit of main channel confluences, and in downstream reaches of the main channel. Deposition in the main channel can impede passage of the reservoir overflow and, by deflecting flow into the channel banks, cause irregular channel widening. Sediment deltas and bars deposited farther downstream can initiate or accelerate erosion of stream banks and levees, impact navigation, endanger ecological balances, and increase the danger of overbank flooding.

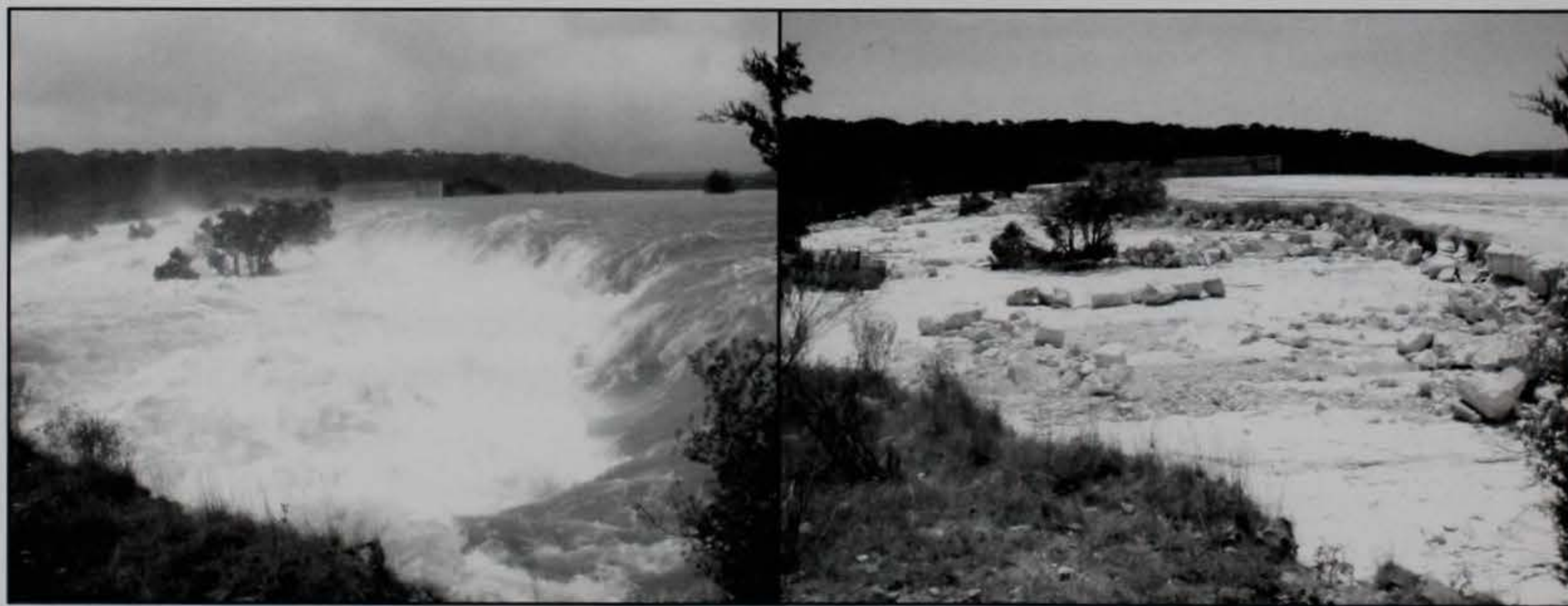


Figure 8. Damage to Canyon Lake Spillway during and after a storm event in July 2002 (photos courtesy USACE District, Fort Worth).

Because of the great uncertainty regarding unlined spillway parameters, it is very important to understand spillway erosion hazards. There is no consensus among experts on the definition of risk; instead, they define it as is appropriate to their specific case. For this research, risk assessment is defined as a process of answering three questions: (1) what can go wrong, (2) what is the likelihood it will go wrong, and (3) what are the consequences if it does go wrong.

In the case of unlined spillway erosion, the answer to the first question is that there could be local scouring that can lead to the development of headcut and possible further damage. An outcome of this erosion process could be breach of the spillway and possibly the dam itself, if the spillway is located near the main dam body. The primary goal of this research is to answer the second question by quantifying the likelihood of something going wrong with the spillway, specifically erosional damage. The consequences of spillway damage involve its repair cost, which depends on the level of damage: slight, moderate, or severe. A spillway breach as a result of damage involves the population at risk and/or loss of economic value in the downstream area.

This research intends to contribute to the advancement of spillway erosion evaluation. This will be accomplished through the development of spillway erosion damage prediction that assists in the clarification of the uncertainties dictated by the variability in the channel geometry, geologic materials, and flood discharge. This risk assessment analysis plan will give a better understanding of the behavior of unlined rock surface spillways.

4 Methodology

Parametric study data and SSEA

The parametric analysis conducted in this research was done using the SSEA (v. 2004) software. To use the SSEA software effectively, three steps are required. All three steps can be completed within the integrated development environment. In the first step, a user creates an input file containing spillway geometry, geologic material properties of the analyzed spillway and the hydrographs routed through the spillway. In the second step, the input file is processed to simulate the erosion that occurs when the hydrograph is routed through the spillway. In the third and final step, the output can be analyzed in both text and graphical format.

Table 8 contains a list of the required input parameters. Although all of them are required, their individual impact on the results is different. As part of this study, each input parameter was tested individually to recognize the impact or the sensitivity of the results to changes from the specific parameter. The action column in Table 8 addresses which of the parameter values stayed constant through the study.

Influence of particle diameter in vertical erosion

As was mentioned in Chapter 2, the vertical erosion in Phases 2 and 3 (headcut deepening in Phase 3) uses Figure 2, developed from the Shields diagram, as the threshold line in defining the initiation of vertical erosion. The abscissa in the graph is particle diameter in inches that describes the properties of material in resisting erosion. For soil materials, the particle diameter is defined as D_{75} , the diameter for which 75% of the material is smaller. For rock material, particle diameter can be obtained from Equation 20 when the values of RQD are available, or by using Equation 21 when joint spacing in three orthogonal directions is available from site evaluation. While conducting this study, it was discovered that the diameter of the geologic material had certain sensitivity which needed to be considered in the parametric study efforts. Over 80 cases from different sources were collected to compare the variability of erodibility index with the material diameter. Table 9 gives examples of the erosion index (K_h) calculations for different geologic materials. Some of these values were

Table 8. SSEA input interface parameters.

Screen Title	Parameter (units)	Action
Watershed Information	Watershed ID	
AS Hydrograph Data	Time (hr)	Varies
	Discharge (cfs)	Varies
AS Surface Profile	Enter AS Surface Profile	Not Selected
	Profile Defined by Material Coordinates	Selected
AS Surface Parameters	Side Slope Ratio	1
	Bottom Width (ft)	300
	Elevation Valley Floor (ft)	100
	Reach Station Beginning (ft)	Varies
	Reach Station Ending (ft)	Varies
	Vegetal Retardance Curve Index	4
	Vegetal Cover Factor	0.5
	Maintenance Code	2
	Potential Root Depth (ft)	
AS Material Properties and Coordinates	Plasticity Index	0
	Dry Density (lcf)	130, 160
	Headcut Index	Varies
	Percent Clay	0
	Representative Diameter (in.)	Varies
	Coordinates: Station (ft) Elevation (ft)	Varies
Cont. Headcut Model Selection	USDA	Selected
	USACE	Not Selected
	Crest Barrier	Not Selected
	Barrier	Not Selected
AS = Auxiliary Spillway		

Table 9. Examples of erosion index values for some geologic materials.

Geologic Material	Erosion Index (K_h)
ML	0.02
CL	0.1
Shale	0.5
Shaley Limestone	13
Sandstone	20
Siltstone	640
Sandstone (BD)	974
Limestone (Rip-Rap)	1,218
Glenrock Limestone	2,478
Dolomite	10,240
Ryolite	35,000

collected from previous data available from the USDA or calculated as part of this study.

Figure 9 shows the relation between Erosion Index K_h in horizontal axis and particle diameter in vertical axis that are calculated during case history evaluations from USACE and USDA. Although the relation is not strong, Figure 9 may be used as a rough check on the consistency of input parameters used in model application. Thus, the diameter values for this parametric study were calculated using the equation:

$$\log Y = 0.295913 (\log K_h) + 0.712322 \quad (26)$$

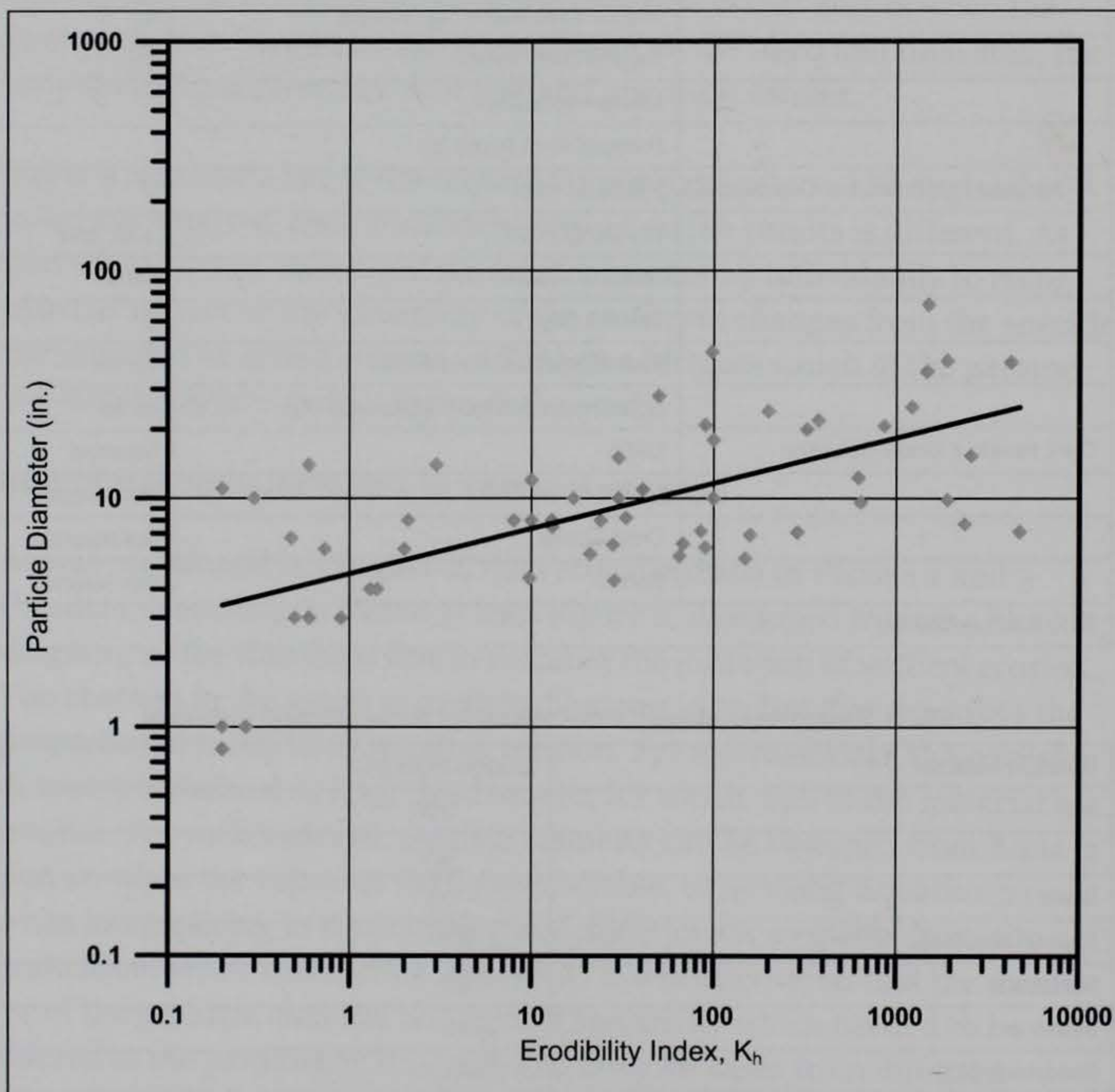


Figure 9. Relationship between erodibility index and particle diameter.

Parameters selection

The variables and boundaries selection for this study was based on historic data collected by the USDA through the years and some USACE cases. These data were put to the test in the original SITES and then transitioned into the SSEA program. A list of the parameters and respective screens can be seen in Table 8. Many parameter testing attempts were made using the program to get to conclusions on the most influential input data while at the same time assisting in the improvement of the program. Based on this testing it was concluded that there were five parameters to be used for the study. These parameters demonstrated the most influence and impact on the results. For the geometry of the spillway there are two parameters that help define the spillway shape: the length and the slope. The length of the spillway ranged from 400 ft for a short spillway (Blue River, OK) to 3000 ft for a longer spillway (Tuttle Creek, KS). Their slopes ranged from 1 to 20 deg, where half of the cases had a single spillway and the other half were tested using a two slope spillway. For spillways with two slopes, an average slope was used. Since this practice can be a new challenge in spillway erosion research, currently there is research being conducted to achieve a better understanding of multi-slope behavior using the SSEA program. The width of the spillway stayed constant at 300 ft. For the hydrology, the parameters that control the output results are the peak discharge and the duration. These values range from a peak discharge of 4,000 to 60,000 cfs. The duration of the discharge ranges from 10 hr to 300 hr.

There are five factors that describe the geologic material properties. Of these five, only two parameters were considered to have a significant impact in the test results: the diameter and K_h . The other three remained constant. As mentioned in the previous section, testing conducted to detect the effect of these parameters in the spillway erosion results demonstrated that the diameter of the geologic material has a great influence in the spillway output results. Then, data analysis was conducted using USDA and USACE historic data to have more accurate diameter values that will relate accurately with the erosion index. The results of this study were expressed in the previous section. The headcut erosion index (K_h) had values ranging from 10, for a low erosion resistant rock, to 10,000 for a higher erosion resistant rock, and diameter sizes ranging from 10.2 in. to 78.7 in.

Table 10 summarizes the data values used for each parameter. A combination of these parameters was done and the results calculated using the SITES and, later, the SSEA program. A code was used with each parameter to facilitate its recognition and for file name purposes, because hundreds of trials were performed (Example: G1H2M3). Not all parameter combinations were done for this study due to time restrictions caused by file conversions. Data used for the calculations, a total of 275 combinations, are shown in Appendix A.

Table 10. Variables used for the parametric studies and their values.

Geometry			Hydrology			Geology Material		
Code	Slope (deg)	Length (ft)	Code	Peak Discharge (cfs)	Duration (hr)	Code	Diameter (in.)	K _n
G2	5	400	H1	4000	10	M1	10.2	10
G5	5	1000	H2	4000	300	M3	20.1	100
G1	1	3000	H5	4000	100	M4	32.4	500
G4	5/20	400	A1	10000	10	M2	48.9	2000
G3	5/20	3000	A2	10000	300	M5	78.7	10000
			A3	10000	100			
			B1	20000	10			
			B2	20000	300			
			B3	20000	100			
			C1	40000	10			
			C2	40000	300			
			C2	40000	100			
			H3	60000	10			
			H4	60000	300			
			H6	60000	100			

Summary of examples using SSEA

The spillway damages are defined as the percentage of eroded area compared to the total longitudinal section of the spillway. Three different levels of spillway damages are defined as follows: (1) no damage to light damage when the erosion occurs between 0 and 30%, (2) moderate damage when the erosion ranges from 30.1 to 70%, and (3) severe damage to breach when erosion above 70.1% occurs. An example for each one of the levels is shown in Figures 10, 11, and 12. Each example shows the values used for the test and the percentage of material eroded. The shaded portion represents the percentage of material eroded from the spillway.

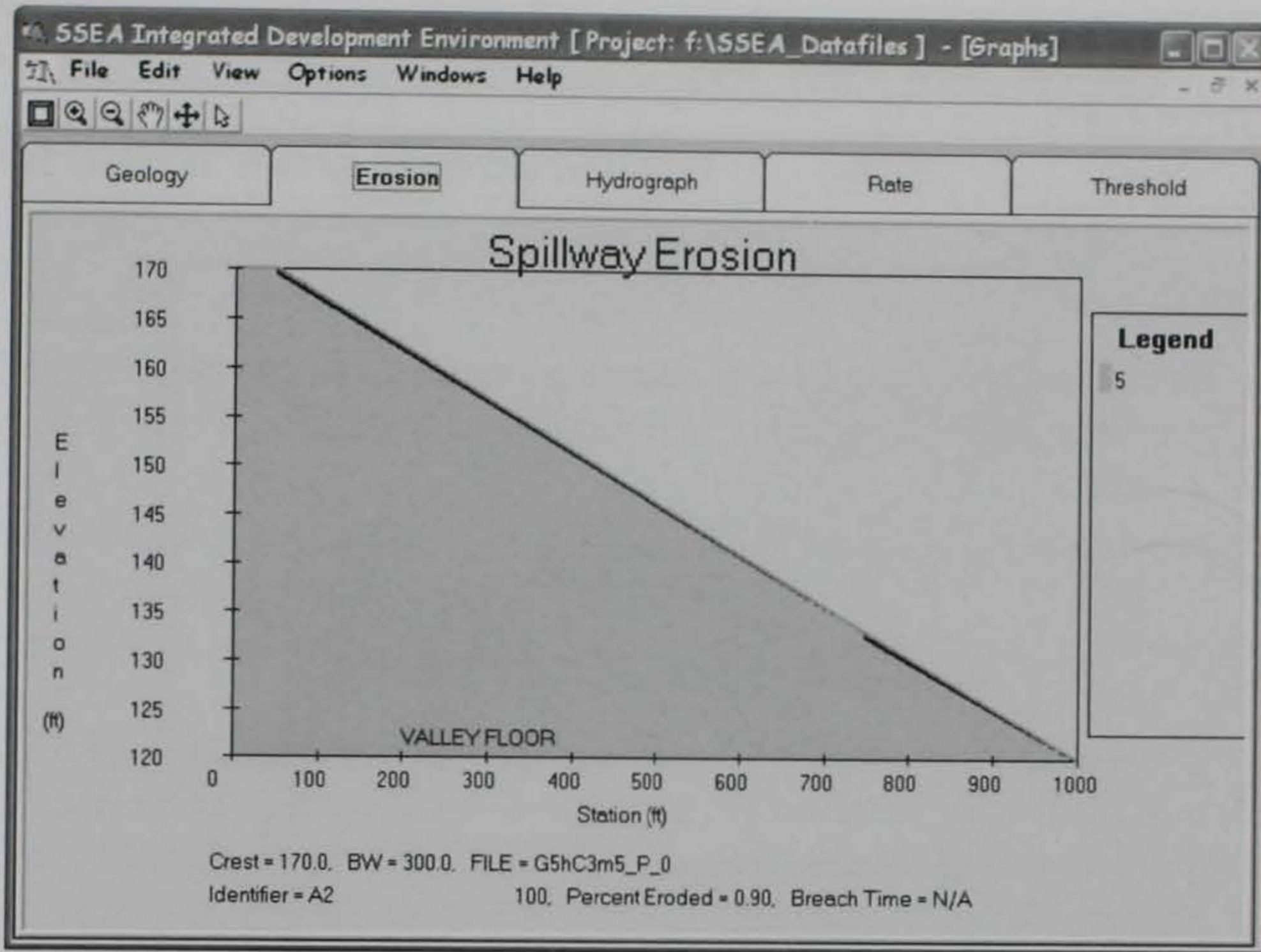


Figure 10. SSEA erosion results with no to light damage to the spillway (0.9% of the material was removed).

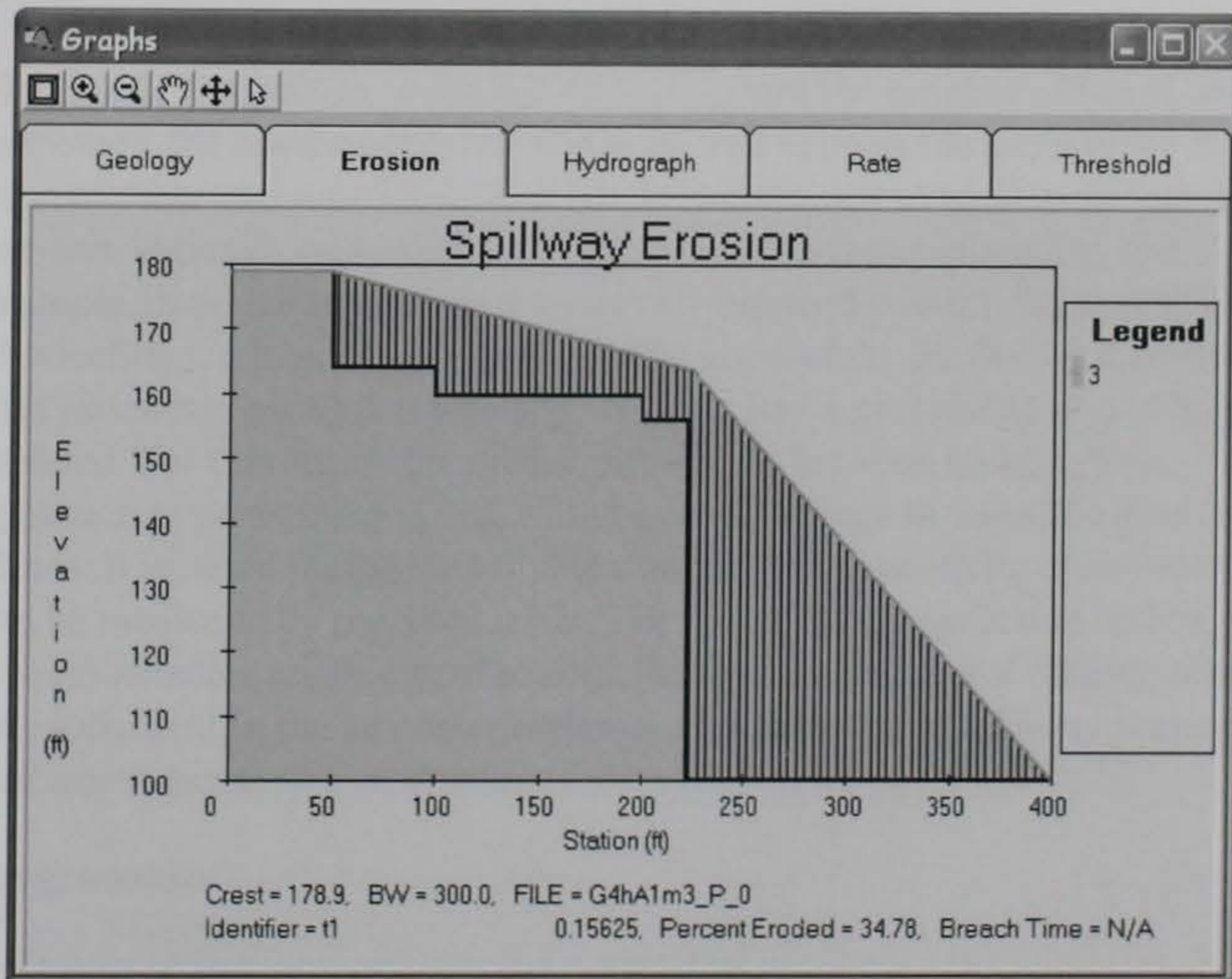


Figure 11. SSEA erosion results with moderate damage to the spillway (34.78% of the material was removed).

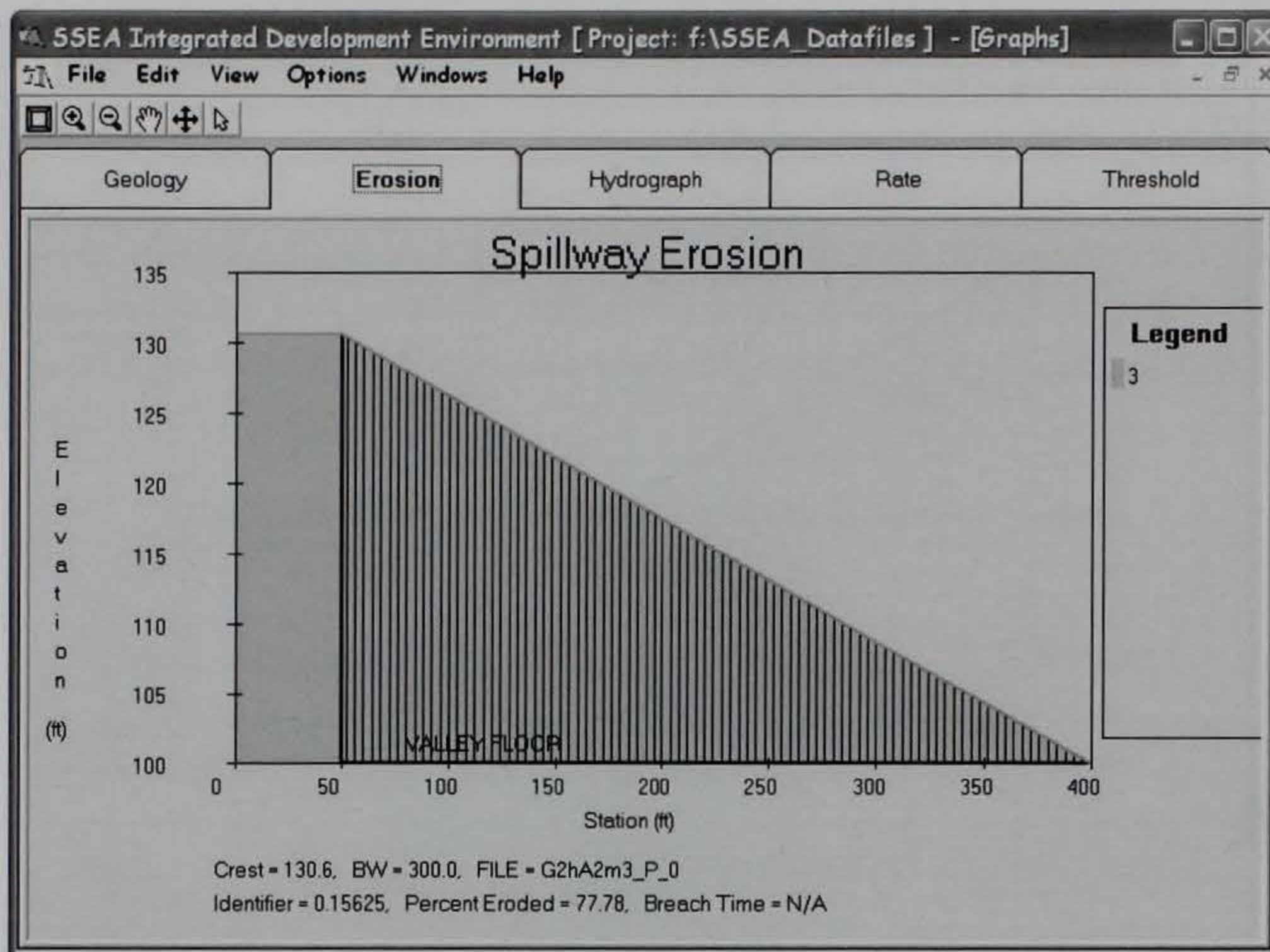


Figure 12. SSEA erosion results showing the spillway breached (77.78% of the material was removed).

5 Results and Discussion

Probability

The probability theory measures, mathematically, the likelihood of an occurrence. Probability of an outcome can be defined as the number of favorable outcomes divided by the total number of possible outcomes. A probability is a real number and is usually given as a percentage between 0% and 100%. A probability of 100% means that an event is certain, whereas a probability of 0% is often taken to mean the event is impossible. For example, a meteorologist might say there is a 60% chance that it will rain tomorrow. This means that in 6 of every 10 times when the world is in the current state, it will rain. Another way of referring to probabilities is odds. The odds of an event are defined as the ratio of the probability that the event occurs to the probability that it does not occur. For example, the odds of a coin landing on a given side are usually written "1 to 1" or "1:1." This means that on average, the coin will land on that side as many times as it will land on the other side.

The classical approach to probability is to count the number of favorable outcomes, the number of total outcomes, and express the probability as a ratio of these two numbers. However, it is necessary to make a distinction between logically impossible and occurring with zero probability. For example, in selecting a number uniformly between 0 and 1, the probability of selecting $1/2$ is 0, but it is not logically impossible. Further, it is certain that whichever number is selected will have had a probability of 0 of being selected. For this study, the probability will be between 0 and 1. This approach to probability is well suited to a wide range of scientific disciplines. It is based on the idea that the underlying probability of an event can be measured by repeated trials. The statistical methods that will be described below are designed to contribute to the process of making scientific judgment in the face of uncertainty and variation in spillway erosion risk assessment.

Linear regression

In statistics, linear regression is a method of estimating the conditional expected value of one variable, y , given the values of some other variable

or variables, x . The variable of interest, y , is conventionally called the response variable. The terms endogenous variable and output variable are also used. The other variables, x , are called the explanatory variables. The terms dependent and independent variables are also used, although it is recommended to be avoided as the variables are not necessarily statistically independent. The explanatory and response variables may be scalars or vectors. This method is used to solve problems involving a set of variables or parameters when it is known that some inherent relationship exists among them. The variables or parameters used for this analysis are mentioned in Section 4. Multiple regression includes cases with more than one explanatory variable. The term explanatory variable suggests that its value can be chosen at will and the response variable is an effect, i.e., causally dependent on the explanatory variable.

Regression, in general, is the problem of estimating a conditional expected value. Linear regression is called linear because the relation of the response to the explanatory variables is assumed to be a linear function of some parameters. In most applications of regression, the linear equation

$$y = \alpha + \beta x \quad (27)$$

is an approximation that is a simplification of something unknown and much more complicated. In the above equation, α and β are the intercept and slope parameters, respectively. Regression models, which are not a linear function of the parameters, are called nonlinear regression models. A neural network is an example of a nonlinear regression model.

Still more generally, regression may be viewed as a special case of density estimation. The joint distribution of the response and explanatory variables can be constructed from the conditional distribution of the response variable and the marginal distribution of the explanatory variables. In some problems, it is convenient to work in the other direction; from the joint distribution, the conditional distribution of the response variable can be derived. Figure 13 depicts the nature if hypothetical x and y data are scattered around a true regression line for a case in which only five observations are available ($n = 5$).

It is necessary to fit the estimated regression line to the data. This allows for the computation of predicted values from the fitted line in Equation 27 and the other types of analysis that will ascertain the strength of the

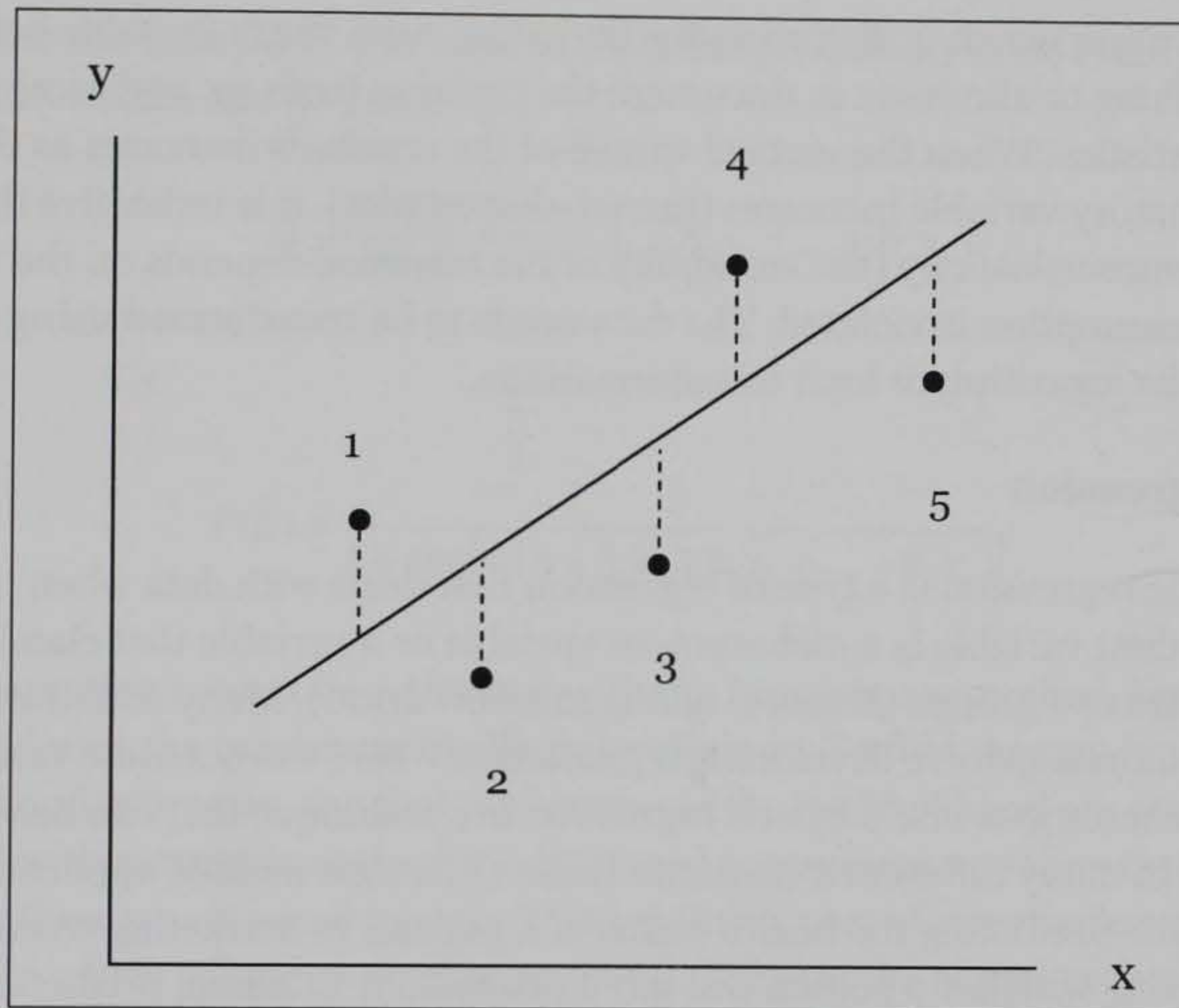


Figure 13. Hypothetical (y,x) data scattered around the true regression line for $n = 5$ (modified after Walpole et al. 2002).

relationship and the adequacy of the fitted model. For this, it is necessary to calculate the residual, which is essentially an error in the fit of the regression line.

The first method of displaying the residuals used the histogram or cumulative distribution to depict the similarity (or lack thereof) to a normal distribution. Nonnormality suggests that the model may not be a good summary description of the data. The residuals are plotted against the explanatory variable, x . The fitted line has predicted values as points on the line, and hence, the residuals are vertical deviations from points to the line as seen in Figure 13.

There should be no discernible trend or pattern if the model is satisfactory for these data. Some of the possible problems are residuals increase (or decrease) as the explanatory variable increases indicating mistakes in the calculations. The mistakes need to be found and corrected. Residuals first rise and then fall (or first fall and then rise) indicating that the appropriate model is (at least) quadratic. Adding a quadratic term (and then possibly higher) to the model may be appropriate. If one residual is much larger than the others, this situation suggests that there is one unusual

observation which is distorting the fit. In this case, verify its value before publishing or eliminate it, document the decision to do so, and recalculate the statistics. When the vertical spread of the residuals increases as the explanatory variable increases (funnel-shaped plot), it is indicative that the homoscedasticity (the variability of the response depends on the value of x) assumption is violated. The data needs to be transformed using perhaps the logarithm or logit transformations.

Logistic regression

Logistic regression is a type of regression that deals with data when the dependent variable is a dichotomous variable or a variable that classifies data into two groups (Hosmer and Lemeshow 2000). Many situations in data analysis involve developing a prediction where the outcome variable is a dichotomous one. Logistic regression is a technique that can be very useful in many different situations. These situations include application in medicine predicting the health status of a patient, in marketing research predicting whether a person will buy a product, or in school predicting the success of a student. In the engineering community, earthquake engineering is probably the first to employ logistic regression. Liao et al. (1988) extended the work of Seed et al. (1983) on the liquefaction threshold line. The original liquefaction threshold line was extended to series of threshold lines with different probabilities.

The linear form of a logistic regression relationship does not occur in the scale of the raw data or probability of an event, but in the natural log of odds of the event instead. The general expression of the logistic regression is:

$$\ln(odds) = \alpha + \beta_1 x_1 + \beta_2 x_2 + \dots + \beta_n x_n \quad (28)$$

The terms on the right hand side of equation are the standard terms for the n number of independent variables (x) with its coefficient (β) and the intercept (α) in a regression equation. The left hand side of the equation is the natural log of the odds, which is called a logit. The odds are defined as the ratio of the probability of an occurrence $P(E)$ to the probability of nonoccurrence:

$$odds = \frac{P(E)}{1 - P(E)} \quad (29)$$

Because the interest of this research is in the probability of an event, Equations 28 and 29 can be combined

$$\ln \frac{P(E)}{1-P(E)} = \alpha + \beta_1 x_1 + \beta_2 x_2 + \dots + \beta_n x_n \quad (30)$$

and

$$P(E) = \frac{1}{1 + \exp[-(\alpha + \beta_1 x_1 + \beta_2 x_2 + \dots + \beta_n x_n)]} \quad (31)$$

This equation cannot be estimated with the least-square method, but instead uses the maximum likelihood technique. To find the maximum likelihood estimates, the first derivatives of the log likelihood are computed with respect to each of the estimated parameters and then these derivatives are set equal to zero. This results in a set of simultaneous equations in which solutions need to be found. Because the equations are nonlinear in the parameters, they are solved using an iterative procedure.

In the case of spillway erosion analysis, two parameters are used in both the USDA and Annandale models: Stream Power (SP) and Erodibility Index (K_h). The outcomes from data collections are the occurrence of erosion or the non-occurrence of erosion.

$$P(E) = \frac{1}{1 + \exp[-(\alpha + \beta_1 K_h + \beta_2 SP)]} \quad (32)$$

This equation was used to fit the expanded USDA data of about 100 points resulting in the family of lines for a range of probabilities shown in the previously shown Figure 7. The logistic regression on this USDA data is expressed as:

$$P(E) = \frac{1}{1 + \exp[-(1.171 + 3.9K_h + 3.364SP)]} \quad (33)$$

Figure 14 shows a series of threshold lines with different probabilities of erosion. The middle line is the threshold line with probability of erosion, $P(E)$, 0.5. The lower bound threshold line has $P(E)$ 0.01, and the upper bound threshold line has $P(E)$ 0.99. The original threshold line is quite

close initially with the middle threshold line ($P(E) = 0.5$). Several statistics may be used to evaluate the logistic regression, among others is Cox and Snell's R^2 , which later modified by Nagelkerke's R^2 (SPSS 1999). The use of R^2 , known as the coefficient of determination, is well known in regression analysis. It is defined as the proportion of variance that is explained by the regression model. It is a useful measure of the success of predicting the dependent variable from the independent variables (Nagelkerke 1991). The closer the value of R^2 is to 1, the more accurate your prediction will be. For the expanded USDA data, the Nagelkerke's R^2 is equal to 0.763.

Similarly, using Equation 32 and the Annandale data of about 140 points shown in Figure 6, the resulting family of lines for a range of probabilities is shown in Figure 15. The logistic regression on Annandale's threshold line is expressed as

$$P(E) = \frac{1}{1 + \exp[-(-1.859 + 7.029K_h + 9.798SP)]} \tag{34}$$

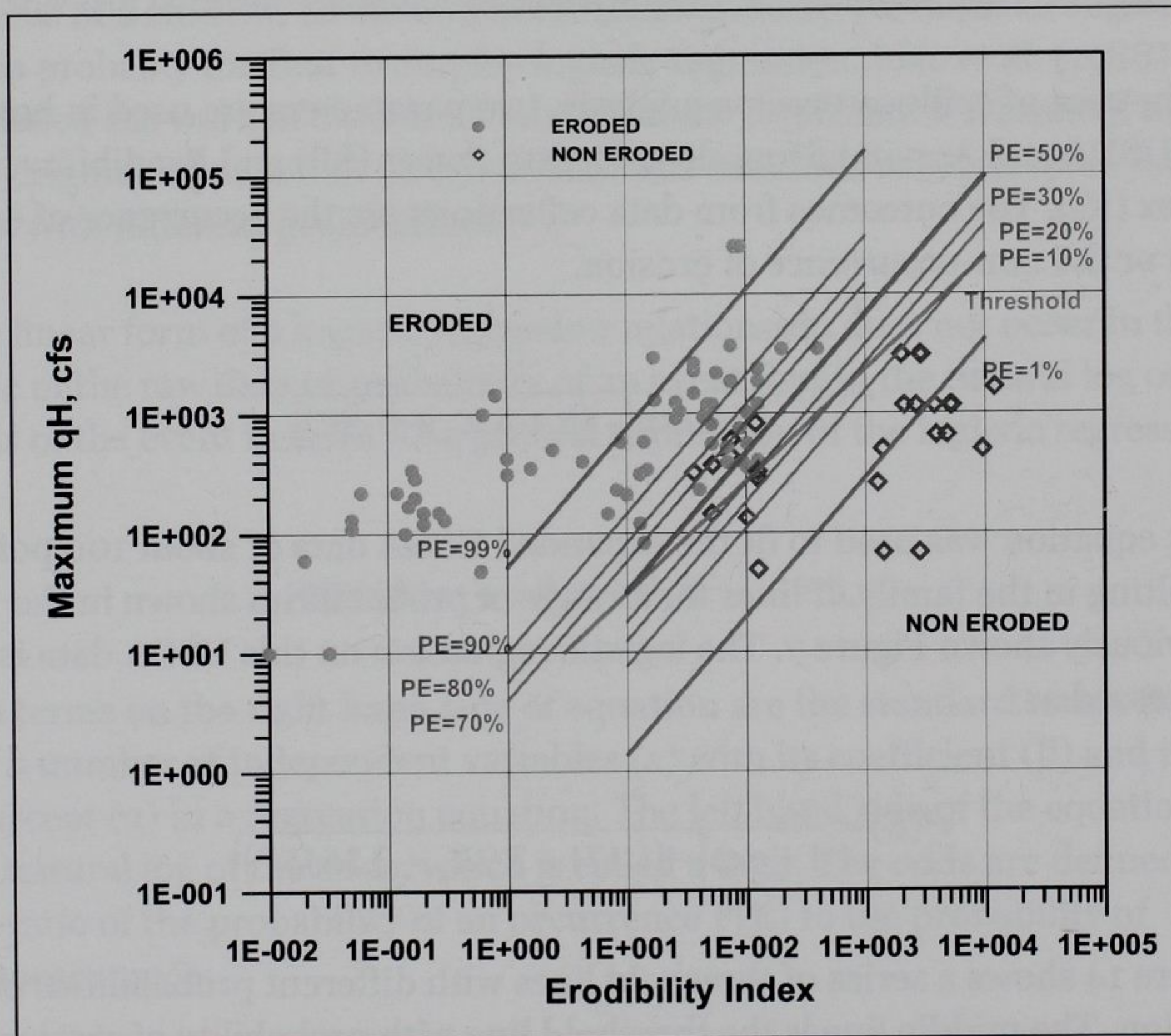


Figure 14. Probability of erosion by logistic regression of case histories (Wibowo and Murphy 2005).

Figure 15 shows three logistic regression lines of Annandale's threshold lines. The upper bound (blue) and lower bound (yellow) have probability collected from previous data available from the USDA or calculated as part of this study.

$P(E) = 0.1$ and $P(E) = 0.99$, respectively. Again, the middle line ($P(E) = 0.5$) (red) is very close to the original threshold line (green) for this data set. The Nagelkerke's R^2 is equal to 0.908.

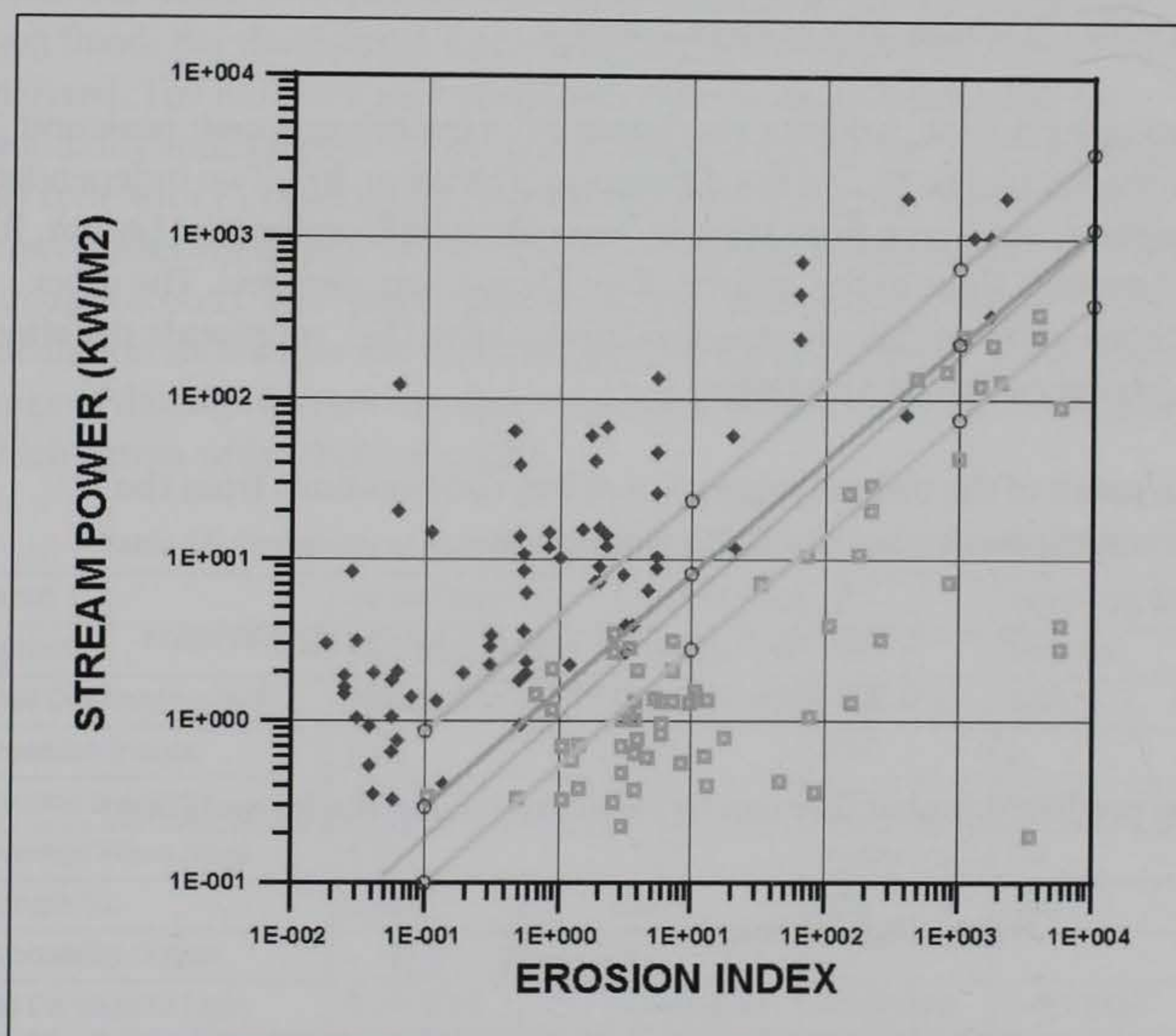


Figure 15. Probability of erosion by logistic regression for Annandale's threshold line (Wibowo and Murphy 2005).

Ordinal regression

For a situation with more than two outcomes, a dichotomous model can be extended to a polytomous model. If the multiple outcomes have no inherent order, the analysis can be done using polytomous logistic regression. Multiple outcomes with inherent order can be analyzed using ordinal logistic regression. This model can be defined equivalently in terms of the odds of an inequality. For certain cutpoints, g , in the domain

$$P(D \geq g|X) = \frac{1}{1 + \exp\left[-\left(\alpha_g + \sum_{i=1}^p \beta_i X_i\right)\right]} \quad (35)$$

$$\text{odds} = \frac{P(D \geq g|X)}{P(D < g|X)} = \exp\left(\alpha_g + \sum_{i=1}^p \beta_i X_i\right) \quad (36)$$

where $P(D)$ = probability of damage and X = predictor or independent variables (Kleinbaum and Klein 2002).

Two independent variables are chosen from hydrology input: peak unit discharges (q , cfs/ft) and flood duration (*Duration*, hr). Two independent variables are chosen from spillway geometry: spillway length (*Length*, ft) and average slope of the spillway floor (*Slope Avg*, degrees). The other independent variable average, erodibility index (K_h), represents the effect of geologic material properties.

The result of the ordinal regression of 275 combinations from the parametric study gave the following equation:

$$S_j = -2.640 \text{ Log } K_h + 5.469 \text{ Log } q + 1.435 \text{ Log } \textit{Duration} \\ + 0.305 \text{ Slope Avg} - 0.987 \text{ Log } \textit{Length} \quad (37)$$

The predicted probability can be calculated using the formulation:

$$\begin{aligned} \text{No to Slight Damage} &= \frac{1}{(1 + \exp(S_j - k_1))} \\ \text{Moderate Damage} &= \frac{1}{(1 + \exp(S_j - k_2))} - \frac{1}{(1 + \exp(S_j - k_1))} \\ \text{Severe Damage to Breach} &= 1 - \frac{1}{(1 + \exp(S_j - k_2))} \end{aligned} \quad (38)$$

where k_1 and k_2 are boundary parameters from regression, $k_1 = 4.839$, and $k_2 = 6.035$. The Nagelkerke's R^2 is equal to 0.741.

Case history data application

The probability of erosion calculation using Ordinal Logistic Regression was applied on Tuttle Creek Spillway, KS; Painted Rock Spillway, AZ; and

Buck-Doe Spillway, MO (see summary in Table 11). Tuttle Creek Spillway experienced a 100-yr flood with discharge of about 60,000 cfs with 520-hr duration. Results of damage are shown in Figure 16. The length of the spillway is about 2200 ft, the average floor slope is about 1.4 degrees, and the average erodibility index is 17. Table 11 shows that the probability of having severe damage to breach $P(D)$ is 0.986, and $P(D)$ for moderate damage is about 0.008. This result predicts a very small chance that the spillway will breach. The predicted damage is between severe and breached, which is consistent with what actually happened during the 1993 flood. For the Painted Rock Spillway, two longitudinal sections were analyzed. The northern part of spillway floor is intact felsite with an Erodibility Index K_h more than 5000, and the middle section is fractured tuff zone with K_h of about 28. During the 1993 flood, the northern part stayed intact which agrees with the $P(D)$ calculation of no damage to light damage (0.902). The middle part is severely damaged by the flood and the calculation shows that the $P(D)$ is 0.999, which is inside the appropriate range of damage (severe damage to breach). Buck-Doe breached in 3 hr, which agrees with a $P(D)$ of 0.999.

Table 11. Probability of spillway damages using ordinal logistic regression.

Input	Tuttle Creek, KS	Painted Rock, AZ		Buck-Doe, MO
Material	Limestone-Shale	Felsite	Tuff	Soft clay
Unit Discharge (cfs/ft)	112.1	41.8	41.8	163.5
Duration (hours)	520	576	576	3
Erosion Index, K_h	17	5340	28	0.01
Average Slope (deg)	1.4	1.32	14.04	7.2
Length (ft)	2200	520	230	155
Probability Output				
No Damage to Light	0.005861	0.902945	0.000329	0.000000
Moderate	0.008057	0.054087	0.000458	0.000000
Severe to Breach	0.986082	0.042968	0.999213	0.999999

These cases demonstrate that probability calculation using ordinal logistic regression may be used for quick assessments and provides decision-makers with a screening tool to justify remedial actions for a spillway or for a portfolio analysis. However, if the probability outcome raises concern, a more rigorous analysis needs to be done using an appropriate tool.



Figure 16. Tuttle Creek Spillway after being used during the Flood of 1993.

6 Conclusions

The outlet works are critical elements in the safe operation of a dam, and they must be protected from damage that could lead to complete failure from unlined spillway erosion. Another challenge is that the gathering of data is of no use if it lacks scientific interpretation. These needs resulted in developing procedures and tools that support spillway erosion risk assessment with the capability to estimate the probability of erosion and level of damage to earth and rock surface spillways using logistic and ordinal regression techniques. As part of this study, a procedure was developed that compares SSEA damage levels with ordinal logistic regression. The procedure explained in this study was applied to 275 cases developed from a parameters comparison. Of the 275 cases analyzed with the definition of damage, 42 of them, when compared with the ordinal logistic regression, were not equal. This gave 84.7% accuracy. The same procedures have also been applied to case histories to assess their reliability with accurate results. The statistical methods used in this analysis are designed to contribute to the process of making scientific judgment in the face of uncertainty and variation in spillway erosion risk assessment. Although, more rigorous analysis needs to be done, the probability calculations may be used for quick decision making. These risk assessment tools will assist decision makers in justifying any needed maintenance and will be useful tools for screening and portfolio analysis.

References

- Annandale, G. W. 1992. *Determination of the erodibility of the plunge pool under probably maximum flood conditions; Bartlett Dam, Salt River Project, AZ.* Tucson, AZ: Steffen Robertson and Kirsten, Inc.
- Annandale, G. W. 1995. Erodibility. *J. Hydraulic Research, IAHR* 33(4):471-494.
- Annandale, G. W. 2002. The erodibility index method: An overview. *Proceedings, International Workshop on Rock Scour due to Falling High-Velocity Jets, 25-28 September, Lausanne, Switzerland.* Swiss Federal Institute of Technology.
- ASTM International, West Conshohocken, PA.
- D-1194, Standard test method for bearing capacity of soil for static loading and spread footings.
- D-1586-99, Standard test method for penetration test and split-barrel sampling of soils.
- D-2166-06, Standard test method for unconfined compressive strength of cohesive soil.
- D-2573-01, Standard test method for field vane shear test in cohesive soil.
- D-2938-95, Standard test method for unconfined compressive strength of intact rock core (Superseded).
- D-4648-05, Standard test method for laboratory miniature vane shear test for saturated fine-grained clayey soil.
- D-5731-05, Standard test method for determination of the point load strength index of rock.
- Barton, N., R. Lien, and J. Lunde. 1974. Engineering classification of rock masses for the design of tunnel support. *Rock Mechanics* 6:189-236.
- Bollaert, E., and A. Schleiss. 2002. A physically-based engineering model for the evaluation of the ultimate scour depth due to high-velocity jet impact. In *Proceedings, International Workshop on Rock Scour due to High-Velocity Jets, 25-28 September, Lausanne, Switzerland*, 161-174. Swiss Federal Institute of Technology.
- Deere, D. U. 1964. Technical description of rock cores for engineering purposes. *Rock Mech. Engrg. Geol.* 1:17-22.
- Deere, D. V., and D. W. Deere. 1988. The rock quality designation (RQD) index in practice. In *Rock classification systems for engineering purposes.* ASTM STP 984, ed. L. Kirkaldie, 91-101. Philadelphia, PA: American Society for Testing and Materials.

- Fell, R. 1994. Landslide risk assessment and allowable risk. *Canadian Geotechnical Journal* 31(2):261–272.
- Hanson, G. J. 1991. Development of a jet index to characterize erosion resistance of soils in earthen spillways. *Transactions of American Society of Agricultural Engineers* 34(5):2015–2020.
- Hanson, G. J., K. M. Robinson, and K. R. Cook. 1997. Headcut migration analysis of a compacted soil. *Trans. ASAE* 40(2):355–361.
- Hosmer, D. W., and S. Lemeshow. 2000. *Applied logistic regression*. New York: Wiley.
- International Commission on Large Dams. 1998. World register of dams (computerized version). Paris, France.
- Kirsten, H. A. D. 1982. A classification system of excavation in natural materials. *The Civil Engineer in South Africa* 24:292–308.
- Kirsten, H. A. D. 1988. Discussion on rock material field classification procedure. In *Rock classification systems for engineering purposes*. ASTM STP 984, ed. L. Kirkaldie, 55–58. Philadelphia, PA: American Society for Testing and Materials.
- Kleinbaum, D. G., and M. Klein. 2002. *Logistic regression*. New York: Springer Verlag.
- Liao, S. S. C., D. Veneziano, and R. V. Whitman. 1988. Regression models for evaluating liquefaction probability. *Journal of Geotechnical Engineering, ASCE* 114(4), 389–411.
- May, J. H. 1989. *Geotechnical aspects of rock erosion in emergency spillway channels; Report 4, Geologic and hydrodynamic controls on the mechanics of knickpoint migration*. Technical Report REMR-GT-3. Vicksburg, MS: U.S. Army Engineer Waterways Experiment Station.
- May, J. H., J. L. Wibowo, and C. C. Mathewson. 2002. Geotechnical aspect of rock erosion. *Proceedings, International Workshop on Rock Scour due to Falling High-Velocity Jets, 25-28 September, Lausanne, Switzerland*, 175–186. Swiss Federal Institute of Technology.
- Moore, J. S., D. M. Temple, and H. A. D. Kirsten. 1994. Headcut advance threshold in earth spillways. *Bull. of the Assoc. of Engr. Geologists* XXXI(2):277–280.
- Nagelkerke, N. J. D. 1991. A note on a general definition of the coefficient of determination. *Biometrika* 78(3):691–692.
- Seed, H. B., I. M. Idriss, and I. Arango. 1983. Evaluation of liquefaction potential using field performance data. *Jour. Geotech. Engineering, ASCE* 109(3):458–482.
- SPSS, Inc. 1999. *Regression models, V. 10.0*. Chicago, IL.
- Stata Reference Manual. 2000. Release 7, Vol 2. College Station, TX: Stata Press.
- Temple, D. M. 1989. Mechanics of an earth spillway failure. *Trans. ASAE* 32(6):2015–2021.

- Temple, D. M., and G. J. Hanson. 1993. Headcut development in vegetated earth spillways. *International Summer Meeting of ASAE/CSAE, June 20–23, Spokane, WA*, Paper No. 932017.
- Temple, D. M., and J. S. Moore. 1994. Headcut advance prediction for earth spillways. *International Winter Meeting of ASAE, December 13–16, Atlanta, GA*, Paper No. 942540.
- Temple, D. M., J. L. Wibowo, and M. L. Neilsen. 2003. Erosion of earth spillways. *Proc., United States Society on Dams* (CD).
- USACE (U.S. Army Corps of Engineers). 1990. Hydraulic design of spillways. Engineer Manual 1110-2-1603. Washington, DC.
- USACE. 1994. Hydraulic design of flood control channels. Engineer Manual 1110-2-1601. Washington, DC.
- U.S. Department of Agriculture. 1996. SITES: Water resource site analysis computer program user's guide. Washington, DC: Natural Resources Conservation Service.
- U.S. Department of Agriculture. 1997. National engineering handbook; Part 628 Dams; Chapter 51 Earth spillway erosion model. Washington, DC: Natural Resources Conservation Service.
- U.S. Department of Agriculture. 1973. A guide for design and layout of earth emergency spillways as part of emergency spillway systems for earth dams. Technical Release No. 52. Washington, DC: Soil Conservation Service.
- U.S. Society on Dams. 2004. Erosion of unlined spillways. Hydraulics Committee, Chapter 4 (draft). Denver, CO.
- Walpole, R. E., R. H. Myers, S. L. Myers, and K. Ye. 2002. *Probability and statistics for engineers and scientists*. 7th ed. Upper Saddle River, NJ: Pearson Education International.
- Whittman, R. V. 1996. Organizing and evaluating uncertainty in geotechnical engineering. *Uncertainty in the Geologic Environment: From Theory to Practice; Proceedings, Uncertainty '96*, Madison, WI.
- Wibowo, J. L., and W. L. Murphy. 2005. *Unlined spillway erosion prediction model*. Technical Report (unpublished). Vicksburg, MS: U.S. Army Engineer Research and Development Center.
- Wibowo, J. L., E. Villanueva, D. M. Temple, and M. L. Neilsen. 2004. *SITES spillway erosion analysis with Latin hypercube sampling (SSEA+LHS), User manual*. Technical Report (unpublished). Vicksburg, MS: U.S. Army Engineer Research and Development Center.
- Wibowo, J. L., D. E. Yule, E. Villanueva, and D. M. Temple. 2005. Earth and rock surface spillway erosion risk assessment. *U.S. Symposium on Rock Mechanics*, Paper No. 05-813. Alexandria, VA: American Rock Mechanics Association.

Appendix A: Probability of Damage Comparing SSEA and Ordinal Logistic Regression (OLR) Results

File Name	Sj	SSEA Results	No Damage Light (1)	Moderate (2)	Severe Breach (3)	OLR
G1h1m1	1.8198	1	0.953435	0.032011	0.014554	1
G1h2m1	3.9394	1	0.710858	0.179613	0.109530	1
G1h3m1	8.2524	3	0.031879	0.066319	0.901802	3
G1h4m1	10.3721	3	0.003938	0.008968	0.987094	3
G1hA1m1	3.9965	1	0.698998	0.185785	0.115216	1
G1hA2m1	6.1161	1	0.218038	0.261689	0.520273	3
G1hB1m1	5.6432	1	0.309137	0.287589	0.403274	3
G1hB2m1	7.7628	3	0.050988	0.099878	0.849134	3
G1hC1m1	7.2893	3	0.079416	0.142539	0.778045	3
G1hC2m1	9.4090	3	0.010252	0.022867	0.966881	3
G2h1m1	3.9035	1	0.718197	0.175734	0.106069	1
G2h2m1	6.0231	1	0.234310	0.268657	0.497033	3
G2h3m1	10.3361	3	0.004082	0.009290	0.986628	3
G2h4m1	12.4558	3	0.000492	0.001133	0.998375	3
G2hA1m1	6.0802	3	0.224235	0.264478	0.511286	3
G2hA2m1	8.1998	3	0.033543	0.069412	0.897046	3
G2hB1m1	7.7268	3	0.052758	0.102776	0.844466	3
G2hB2m1	9.8465	3	0.006643	0.014993	0.978364	3
G2hC1 m1	9.3730	3	0.010624	0.023667	0.965710	3
G2hC2m1	11.4927	3	0.001288	0.002958	0.995755	3
G3h1m1	4.7173	3	0.530393	0.258409	0.211197	1
G3h2m1	6.8369	3	0.119419	0.190191	0.690391	3
G3h3m1	11.1499	3	0.001813	0.004158	0.994029	3
G3h4m1	13.2696	3	0.000218	0.000503	0.999279	3
G3hA1m1	6.8940	3	0.113551	0.184004	0.702445	3
G3hA2m1	9.0136	3	0.015148	0.033253	0.951600	3
G3hB1m1	8.5407	3	0.024088	0.051375	0.924537	3
G3hB2m1	10.6603	3	0.002955	0.006750	0.990295	3
G3hC1m1	10.1868	3	0.004736	0.010756	0.984508	3
G3hC2m1	12.3065	3	0.000571	0.001315	0.998114	3

File Name	Sj	SSEA Results	No Damage Light (1)	Moderate (2)	Severe Breach (3)	OLR
G4h1m1	6.1910	3	0.205550	0.255538	0.538912	3
G4h2m1	8.3106	3	0.030130	0.063031	0.906839	3
G4h3m1	12.6236	3	0.000416	0.000958	0.998626	3
G4H4M1	14.7433	3	0.000050	0.000115	0.999835	3
G4hA1 m1	8.3677	3	0.028508	0.059947	0.911545	3
G4hA2m1	10.4873	3	0.003511	0.008006	0.988483	3
G4hB1m1	10.0143	3	0.005622	0.012732	0.981645	3
G4hB2m1	12.1340	3	0.000678	0.001562	0.997760	3
G4hC1m1	11.6605	3	0.001089	0.002503	0.996408	3
G4hC2m1	13.7802	3	0.000131	0.000302	0.999567	3
G1h1m2	-4.2549	1	0.999888	0.000078	0.000034	1
G1h1m3	-0.8202	1	0.996527	0.002420	0.001053	1
G1h1m4	-2.6655	1	0.999450	0.000384	0.000166	1
G1h1m5	-6.1002	1	0.999982	0.000012	0.000005	1
G1h2m2	-2.1353	1	0.999065	0.000652	0.000283	1
G1h2m3	1.2994	1	0.971792	0.019506	0.008701	1
G1h2m4	-0.5458	1	0.995435	0.003180	0.001385	1
G1h2m5	-3.9806	1	0.999852	0.000103	0.000045	1
G1h3m2	2.1777	1	0.934704	0.044608	0.020688	1
G1h3m3	5.6124	2	0.315741	0.288361	0.395898	3
G1h3m4	3.7671	1	0.744952	0.161229	0.093819	1
G1h3m5	0.3324	1	0.989084	0.007589	0.003326	1
G1h4m2	4.2974	1	0.632193	0.218194	0.149613	1
G1h4m3	7.7321	3	0.052497	0.102350	0.845153	3
G1h4m4	5.8868	1	0.259647	0.277334	0.463018	3
G1h4m5	2.4521	1	0.915824	0.057133	0.027043	1
G1hA1m2	-2.0783	1	0.999010	0.000690	0.000299	1
G1hA1m3	1.3565	1	0.970187	0.020606	0.009207	1
G1hA1m4	-0.4888	1	0.995169	0.003365	0.001466	1
G1hA1m5	-3.9235	1	0.999844	0.000109	0.000047	1
G1hA2m2	0.0414	1	0.991818	0.005694	0.002489	1
G1hA2m3	3.4761	1	0.796225	0.131942	0.071833	1
G1hA2m4	1.6309	1	0.961140	0.026782	0.012079	1
G1hA2m5	-1.8039	1	0.998698	0.000908	0.000394	1
G1hB1m2	-0.4316	1	0.994886	0.003562	0.001552	1
G1hB1m3	3.0032	1	0.862456	0.091536	0.046008	1
G1hB1m4	1.1579	1	0.975425	0.017014	0.007561	1

File Name	Sj	SSEA Results	No Damage Light (1)	Moderate (2)	Severe Breach (3)	OLR
G1hB1m5	-2.2768	1	0.999189	0.000566	0.000246	1
G1hB2m2	1.6881	1	0.958944	0.028275	0.012781	1
G1hB2m3	5.1228	1	0.429516	0.283929	0.286555	1
G1hB2m4	3.2775	1	0.826562	0.113771	0.059667	1
G1hB2m5	-0.1572	1	0.993282	0.004677	0.002041	1
G1hC1m2	1.2146	1	0.974028	0.017973	0.007999	1
G1hC1m3	4.6493	1	0.547280	0.252623	0.200097	1
G1hC1m4	2.8040	1	0.884420	0.077563	0.038017	1
G1hC1m5	-0.6307	1	0.995805	0.002923	0.001272	1
G1hC2m2	3.3343	1	0.818280	0.118790	0.062930	1
G1hC2m3	6.7690	3	0.126753	0.197569	0.675678	3
G1hC2m4	4.9237	1	0.478838	0.273534	0.247629	1
G1hC2m5	1.4890	1	0.966105	0.023397	0.010498	1
G2h1m2	-2.1713	1	0.999098	0.000629	0.000273	1
G2h1m3	1.2635	1	0.972762	0.018841	0.008396	1
G2h1m4	-0.5818	1	0.995596	0.003068	0.001336	1
G2h1m5	-4.0165	1	0.999857	0.000099	0.000043	1
G2h2m2	-0.0516	1	0.992539	0.005193	0.002268	1
G2h2m3	3.3831	1	0.810900	0.123226	0.065874	1
G2h2m4	1.5379	1	0.964468	0.024514	0.011018	1
G2h2m5	-1.8969	1	0.998814	0.000827	0.000359	1
G2h3m2	4.2614	3	0.640519	0.214388	0.145093	1
G2h3m3	7.6961	3	0.054315	0.105299	0.840386	3
G2h3m4	5.8508	3	0.266624	0.279292	0.454084	3
G2h3m5	2.4161	1	0.918557	0.055331	0.026112	1
G2h4m2	6.3810	3	0.176238	0.238103	0.585659	3
G2h4m3	9.8158	3	0.006849	0.015448	0.977703	3
G2h4m4	7.9705	3	0.041827	0.084317	0.873856	3
G2h4m5	4.5358	1	0.575232	0.242228	0.182540	1
G2hA1m2	0.0054	1	0.992105	0.005494	0.002401	1
G2hA1m3	3.4402	2	0.802001	0.128528	0.069471	1
G2hA1m4	1.5949	1	0.962462	0.025882	0.011657	1
G2hA1m5	-1.8398	1	0.998744	0.000876	0.000380	1
G2hA2m2	2.1251	1	0.937842	0.042510	0.019649	1
G2hA2m3	5.5598	3	0.327212	0.289397	0.383391	3
G2hA2m4	3.7145	1	0.754815	0.155742	0.089443	1
G2hA2m5	0.2798	1	0.989638	0.007206	0.003156	1

File Name	Sj	SSEA Results	No Damage Light (1)	Moderate (2)	Severe Breach (3)	OLR
G2hB1m2	1.6521	1	0.960337	0.027327	0.012335	1
G2hB1m3	5.0868	3	0.438355	0.282390	0.279256	1
G2hB1m4	3.2416	2	0.831660	0.110660	0.057680	1
G2hB1m5	-0.1932	1	0.993518	0.004513	0.001969	1
G2hB2m2	3.7718	1	0.744066	0.161718	0.094216	1
G2hB2m3	7.2065	3	0.085684	0.150898	0.763418	3
G2hB2m4	5.3612	3	0.372331	0.290016	0.337653	1
G2hB2m5	1.9265	1	0.948460	0.035373	0.016167	1
G2hC1m2	3.2983	2	0.823570	0.115589	0.060841	1
G2hC1m3	6.7330	3	0.130789	0.201467	0.667744	3
G2hC1m4	4.8877	3	0.487823	0.271191	0.240986	1
G2hC1m5	1.4530	1	0.967264	0.022605	0.010131	1
G2hC2m2	5.4179	3	0.359175	0.290373	0.350452	1
G2hC2m3	8.8527	3	0.017746	0.038631	0.943623	3
G2hC2m4	7.0074	3	0.102626	0.171780	0.725595	3
G2hC2m5	3.5727	1	0.780114	0.141344	0.078541	1
G3h1m2	-1.3574	1	0.997967	0.001417	0.000616	1
G3h1m3	2.0773	1	0.940572	0.040680	0.018748	1
G3h1m4	0.2320	1	0.990117	0.006874	0.003009	1
G3h1m5	-3.2027	1	0.999678	0.000224	0.000097	1
G3h2m2	0.7622	1	0.983321	0.011576	0.005103	1
G3h2m3	4.1969	2	0.655218	0.207501	0.137282	1
G3h2m4	2.3517	2	0.923249	0.052228	0.024523	1
G3h2m5	-1.0831	1	0.997327	0.001863	0.000810	1
G3h3m2	5.0752	2	0.441224	0.281859	0.276917	1
G3h3m3	8.5099	2	0.024821	0.052814	0.922364	3
G3h3m4	6.6646	2	0.138759	0.208834	0.652406	3
G3h3m5	3.2299	1	0.833284	0.109666	0.057050	1
G3h4m2	7.1949	3	0.086601	0.152091	0.761308	3
G3h4m3	10.6296	3	0.003047	0.006958	0.989995	3
G3h4m4	8.7843	3	0.018978	0.041148	0.939874	3
G3h4m5	5.3496	3	0.375057	0.289890	0.335053	1
G3hA1m2	0.8192	1	0.982359	0.012240	0.005401	1
G3hA1m3	4.2540	1	0.642225	0.213600	0.144176	1
G3hA1m4	2.4087	1	0.919110	0.054966	0.025924	1
G3hA1m5	-1.0260	1	0.997171	0.001972	0.000857	1
G3hA2m2	2.9389	2	0.869901	0.086830	0.043269	1

File Name	Sj	SSEA Results	No Damage Light (1)	Moderate (2)	Severe Breach (3)	OLR
G3hA2m3	6.3736	3	0.177316	0.238824	0.583859	3
G3hA2m4	4.5284	3	0.577042	0.241521	0.181437	1
G3hA2m5	1.0936	1	0.976918	0.015988	0.007094	1
G3hB1m2	2.4659	1	0.914750	0.057840	0.027410	1
G3hB1m3	5.9007	1	0.256993	0.276542	0.466465	3
G3hB1m4	4.0554	1	0.686461	0.192180	0.121359	1
G3hB1m5	0.6207	1	0.985491	0.010077	0.004433	1
G3hB2m2	4.5856	1	0.563012	0.246894	0.190095	1
G3hB2m3	8.0203	3	0.039875	0.080878	0.879248	3
G3hB2m4	6.1750	3	0.208161	0.256885	0.534954	3
G3hB2m5	2.7403	2	0.890774	0.073471	0.035754	1
G3hC1m2	4.1121	2	0.674126	0.198336	0.127538	1
G3hC1m3	7.5468	2	0.062514	0.118156	0.819330	3
G3hC1m4	5.7015	2	0.296811	0.285792	0.417397	3
G3hC1m5	2.2668	1	0.929050	0.048377	0.022573	1
G3hC2m2	6.2318	3	0.198967	0.252000	0.549032	3
G3hC2m3	9.6665	3	0.007943	0.017851	0.974206	3
G3hC2m4	7.8212	3	0.048237	0.095303	0.856461	3
G3hC2m5	4.3865	3	0.611238	0.227453	0.161309	1
G4h1m2	0.1162	1	0.991188	0.006131	0.002681	1
G4h1m3	3.5510	1	0.783815	0.139200	0.076985	1
G4h1m4	1.7057	1	0.958246	0.028748	0.013005	1
G4h1m5	-1.7290	1	0.998597	0.000978	0.000425	1
G4h2m2	2.2359	1	0.931060	0.047039	0.021901	1
G4h2m3	5.6706	1	0.303300	0.286797	0.409903	3
G4h2m4	3.8254	1	0.733734	0.167379	0.098887	1
G4h2m5	0.3906	1	0.988438	0.008037	0.003525	1
G4h3m2	6.5489	2	0.153179	0.221105	0.625716	3
G4h3m3	9.9836	3	0.005797	0.013120	0.981083	3
G4h3m4	8.1383	3	0.035595	0.073180	0.891225	3
G4h3m5	4.7036	1	0.533798	0.257274	0.208928	1
G4H4M2	8.6685	3	0.021258	0.045752	0.932990	3
G4H4M3	12.1033	3	0.000700	0.001610	0.997690	3
G4h4m4	10.2580	3	0.004412	0.010031	0.985557	3
G4H4M5	6.8233	1	0.120865	0.191676	0.687459	3
G4hA1m2	2.2929	1	0.927309	0.049535	0.023156	1
G4hA1m3	5.7277	2	0.291388	0.284850	0.423762	3

File Name	Sj	SSEA Results	No Damage Light (1)	Moderate (2)	Severe Breach (3)	OLR
G4hA1m4	3.8824	1	0.722446	0.173468	0.104086	1
G4hA1m5	0.4477	1	0.987767	0.008502	0.003731	1
G4hA2m2	4.4126	1	0.605013	0.230112	0.164875	1
G4hA2m3	7.8473	3	0.047051	0.093306	0.859642	3
G4hA2m4	6.0020	1	0.238115	0.270124	0.491761	3
G4hA2m5	2.5673	1	0.906504	0.063250	0.030246	1
G4hB1m2	3.9396	1	0.710821	0.179632	0.109547	1
G4hB1m3	7.3743	3	0.073417	0.134201	0.792382	3
G4hB1m4	5.5291	2	0.334019	0.289834	0.376146	3
G4hB1m5	2.0943	1	0.939611	0.041324	0.019065	1
G4hB2m2	6.0593	1	0.227885	0.266042	0.506073	3
G4hB2m3	9.4940	3	0.009424	0.021077	0.969499	3
G4hB2m4	7.6487	2	0.056801	0.109271	0.833929	3
G4hB2m5	4.2140	1	0.651352	0.209332	0.139315	1
G4hC1m2	5.5858	2	0.321524	0.288930	0.389546	3
G4hC1m3	9.0205	3	0.015046	0.033040	0.951915	3
G4hC1m4	7.1752	3	0.088168	0.154113	0.757719	3
G4hC1m5	3.7405	1	0.749979	0.158441	0.091579	1
G4hC2m2	7.7054	3	0.053837	0.104527	0.841635	3
G4hC2m3	11.1402	3	0.001831	0.004198	0.993971	3
G4hC2m4	9.2949	3	0.011477	0.025496	0.963027	3
G4hC2m5	5.8602	1	0.264800	0.278797	0.456403	3
G5h1m1	3.5107	1	0.790560	0.135268	0.074172	1
G5h1m2	-2.5640	1	0.999391	0.000425	0.000184	1
G5h1m3	0.8707	1	0.981445	0.012870	0.005685	1
G5h1m4	-0.9746	1	0.997022	0.002075	0.000902	1
G5h1m5	-4.4093	1	0.999904	0.000067	0.000029	1
G5h2m1	5.6304	1	0.311876	0.287925	0.400199	3
G5h2m2	-0.4444	1	0.994950	0.003517	0.001532	1
G5h2m3	2.9904	1	0.863967	0.090584	0.045450	1
G5h2m4	1.1451	1	0.975729	0.016805	0.007466	1
G5h2m5	-2.2896	1	0.999199	0.000559	0.000242	1
G5h3m1	9.9433	3	0.006034	0.013645	0.980321	3
G5h3m2	3.8686	1	0.725196	0.171994	0.102810	1
G5h3m3	7.3033	3	0.078397	0.141146	0.780457	3
G5h3m4	5.4581	3	0.349997	0.290368	0.359635	3
G5h3m5	6.8513	1	0.117916	0.188631	0.693453	3

File Name	Sj	SSEA Results	No Damage Light (1)	Moderate (2)	Severe Breach (3)	OLR
G5h4m1	12.0630	3	0.000728	0.001676	0.997595	3
G5h4m2	5.9883	1	0.240620	0.271057	0.488323	3
G5h4m3	9.4230	3	0.010111	0.022562	0.967327	3
G5h4m4	7.5777	3	0.060727	0.115413	0.823860	3
G5h4m5	4.1430	1	0.667300	0.201683	0.131017	1
G5h5m1	4.9457	1	0.473351	0.274899	0.251749	1
G5h5m2	-1.1290	1	0.997447	0.001779	0.000773	1
G5h5m3	2.3057	1	0.926444	0.050110	0.023447	1
G5h5m4	0.4604	1	0.987612	0.008609	0.003779	1
G5h5m5	-2.9743	1	0.999596	0.000282	0.000122	1
G5h6m1	11.8103	3	0.000938	0.002156	0.996906	3
G5h6m2	5.7356	1	0.289751	0.284546	0.425702	3
G5h6m3	9.1703	3	0.012980	0.028694	0.958326	3
G5h6m4	7.3250	3	0.076843	0.139004	0.784152	3
G5h6m5	3.8903	1	0.720851	0.174320	0.104829	1
G5hA1m1	5.6874	1	0.299771	0.286267	0.413961	3
G5hA1m2	-0.3873	1	0.994656	0.003722	0.001622	1
G5hA1m3	3.0474	1	0.857125	0.094886	0.047989	1
G5hA1m4	1.2021	1	0.974342	0.017758	0.007901	1
G5hA1m5	0.7284	1	0.983867	0.011199	0.004934	1
G5hA2m1	7.8071	3	0.048890	0.096397	0.854713	3
G5hA2m2	1.7323	1	0.957167	0.029481	0.013352	1
G5hA2m3	5.1671	1	0.418714	0.285604	0.295682	1
G5hA2m4	3.3218	1	0.820130	0.117673	0.062197	1
G5hA2m5	-0.1129	1	0.992980	0.004887	0.002133	1
G5hA3m1	7.1224	3	0.092508	0.159602	0.747889	3
G5hA3m2	1.0477	1	0.977932	0.015290	0.006778	1
G5hA3m3	4.4824	1	0.588220	0.237070	0.174709	1
G5hA3m4	2.6371	1	0.900420	0.067219	0.032361	1
G5hA3m5	-0.7976	1	0.996448	0.002475	0.001077	1
G5hB1m1	7.3341	3	0.076204	0.138117	0.785679	3
G5hB1m2	1.2594	1	0.972871	0.018767	0.008362	1
G5hB1m3	4.6941	3	0.536168	0.256474	0.207358	1
G5hB1m4	2.8488	1	0.879765	0.080547	0.039688	1
G5hB1m5	-0.5859	1	0.995614	0.003056	0.001330	1
G5hB2m1	9.4537	3	0.009808	0.021907	0.968285	3
G5hB2m2	3.3790	1	0.811529	0.122849	0.065622	1

File Name	Sj	SSEA Results	No Damage Light (1)	Moderate (2)	Severe Breach (3)	OLR
G5hB2m3	6.8137	3	0.121880	0.192710	0.685409	3
G5hB2m4	4.9685	1	0.467679	0.276258	0.256062	1
G5hB2m5	1.5337	1	0.964609	0.024418	0.010973	1
G5hB3m1	8.7691	3	0.019264	0.041729	0.939008	3
G5hB3m2	2.6944	1	0.895167	0.070630	0.034203	1
G5hB3m3	6.1291	3	0.215840	0.260658	0.523502	3
G5hB3m4	4.2838	1	0.635342	0.216762	0.147895	1
G5hB3m5	0.8491	1	0.981835	0.012601	0.005564	1
G5hC1m1	8.9802	3	0.015654	0.034308	0.950038	3
G5hC1m2	2.9055	1	0.873635	0.084458	0.041907	1
G5hC1m3	6.3402	3	0.182242	0.242037	0.575721	3
G5hC1m4	4.4949	1	0.585174	0.238298	0.176528	1
G5hC1m5	1.0602	1	0.977660	0.015478	0.006863	1
G5hC2m1	11.0999	3	0.001906	0.004369	0.993725	3
G5hC2m2	5.0252	1	0.453589	0.279396	0.267015	1
G5hC2m3	8.4599	3	0.026061	0.055232	0.918706	3
G5hC2m4	6.6146	3	0.144845	0.214175	0.640980	3
G5hC2m5	2.1929	1	0.933770	0.045232	0.020998	1
G5hC3m1	10.4152	3	0.003773	0.008595	0.987632	3
G5hC3m2	4.3405	1	0.622104	0.222709	0.155186	1
G5hC3m3	7.7752	3	0.050391	0.098892	0.850716	3
G5hC3m4	5.9299	3	0.251439	0.274799	0.473762	3
G5hC3m5	2.4952	1	0.912438	0.059361	0.028202	1

Note: Red font indicates that the SSEA and OLR results are different.

